Massive Ca-induced Membrane Fusion and Phospholipid Changes Triggered by Reverse Na/Ca Exchange in BHK Fibroblasts

Alp Yaradanakul,[1] Tzu-Ming Wang,[1] Vincenzo Lariccia,[1] Mei-Jung Lin,[1] Chengcheng Shen,[1] Xinran Liu,[2] and Donald W. Hilgemann[1]

[1]Department of Physiology and [2]Department of Neuroscience, University of Texas Southwestern Medical Center at Dallas, Dallas, TX 75390

Baby hamster kidney (BHK) fibroblasts increase their cell capacitance by 25–100% within 5 s upon activating maximal Ca influx via constitutively expressed cardiac Na/Ca exchangers (NCX1). Free Ca, measured with fluo-5N, transiently exceeds 0.2 mM with total Ca influx amounting to ~5 mmol/liter cell volume. Capacitance responses are half-maximal when NCX1 promotes a free cytoplasmic Ca of 0.12 mM (Hill coefficient ≈ 2). Capacitance can return to baseline in 1–3 min, and responses can be repeated several times. The membrane tracer, FM 4-64, is taken up during recovery and can be released at a subsequent Ca influx episode. Given recent interest in signaling lipids in membrane fusion, we used green fluorescent protein (GFP) fusions with phosphatidylinositol 4,5-bisphosphate ($PI(4,5)P_2$) and diacylglycerol (DAG) binding domains to analyze phospholipid changes in relation to these responses. $PI(4,5)P_2$ is rapidly cleaved upon activating Ca influx and recovers within 2 min. However, $PI(4,5)P_2$ depletion by activation of overexpressed hM1 muscarinic receptors causes only little membrane fusion, and subsequent fusion in response to Ca influx remains massive. Two results suggest that DAG may be generated from sources other than PI(4,5)P in these protocols. First, acylglycerols are generated in response to elevated Ca, even when $PI(4,5)P_2$ is metabolically depleted. Second, DAG-binding C1A-GFP domains, which are brought to the cell surface by exogenous ligands, translocate rapidly back to the cytoplasm in response to Ca influx. Nevertheless, inhibitors of PLCs and cPLA2, $PI(4,5)P_2$-binding peptides, and PLD modification by butanol do not block membrane fusion. The cationic agents, FM 4-64 and heptalysine, bind profusely to the extracellular cell surface during membrane fusion. While this binding might reflect phosphatidylserine (PS) "scrambling" between monolayers, it is unaffected by a PS-binding protein, lactadherin, and by polylysine from the cytoplasmic side. Furthermore, the PS indicator, annexin-V, binds only slowly after fusion. Therefore, we suggest that the luminal surfaces of membrane vesicles that fuse to the plasmalemma may be rather anionic. In summary, our results provide no support for any regulatory or modulatory role of phospholipids in Ca-induced membrane fusion in fibroblasts.

The Journal of General Physiology

INTRODUCTION

Eukaryotic cells use precisely orchestrated membrane fusion and fission events to perform multiple cell functions (Mayer, 2002; Bankaitis and Morris, 2003; Howell et al., 2006). Fusion events in the secretory pathway are under the control of protein–protein interactions of SNAREs and associated proteins that are the subject of intense ongoing investigation (Koumandou et al., 2007). Among fusion events, the release of neurotransmitters from neurons attracts the most attention owing to its fast triggering by Ca binding to synaptotagmins (Geppert et al., 1994) and to its fundamental role in neuronal signaling (Katz, 2003). It is less well appreciated that other cell types use Ca-activated fusion processes for other functions (Breitbart and Spungin, 1997; Gundersen et al., 2002; Steinhardt, 2005; Czibener et al., 2006), and that those mechanisms allow analysis of the membrane specificity of fusion processes, the physical basis of membrane mixing during fusion, and the nature of sensors that initiate fusion. Even in neurons, asynchronous neurotransmitter release appears to be controlled by Ca sensors that are different from those used in fusion events closely coupled to Ca influx (Maximov and Sudhof, 2005; Sun et al., 2007). Of most interest for this article, many eukaryotic cells employ Ca-triggered membrane fusion as part of a membrane repair reaction initiated by Ca influx through cell surface wounds (Togo et al., 2000; Reddy et al., 2001; Steinhardt, 2005). Standard cell culture fibroblasts, such as CHO cells, can rapidly expand their surface membranes via membrane fusion in response to a large increase of cytoplasmic Ca (Coorssen et al., 1996).

The cytoplasmic Ca concentrations needed to trigger the cell wound response are evidently higher than those needed for neurotransmitter release (Schneggenburger and Neher, 2005). In fibroblasts, fusion appears to be initiated in the range of 10–30 μM free Ca (Coorssen

Correspondence to Donald Hilgemann: donald.hilgemann@utsouthwestern.edu

Abbreviations used in this paper: AMP-PNP, adenosine 5′-(β,γ-imido) triphosphoate; BHK, baby hamster kidney; DAG, diacylglycerol; $PI(4,5)P_2$, phosphatidylinositol 4,5-bisphosphate; PS, phosphatidylserine.

The Rockefeller University Press $30.00
J. Gen. Physiol. Vol. 132 No. 1 29–50
www.jgp.org/cgi/doi/10.1085/jgp.200709865

et al., 1996). In sea urchin eggs, the threshold Ca concentration is ~3 mM (Terasaki et al., 1997), just a few fold less than the Ca concentration of sea water. This Ca sensitivity is low enough so that Ca binding by anionic phospholipids, such as phosphatidylserine (PS) (Wilschut et al., 1981; Papahadjopoulos et al., 1990) and $PIP(4,5)P_2$ (Toner et al., 1988), might in principle play a triggering role, as described for pure phospholipid vesicles (Fraley et al., 1980; Wilschut et al., 1981). As stressed by others, however, Mg does not substitute for Ca in the cell wound response (Steinhardt et al., 1994; Steinhardt, 2005), whereas Mg binds nearly as well to anionic membranes as Ca until the vesicles are brought into close proximity (Feigenson, 1986, 1989). Work in diverse cell types suggests, overall, that the cell wound response involves both SNAREs and synaptotagmins that are related to those underlying neurotransmitter release, albeit with a complication that the wound response can probably involve multiple membrane types, including endosomes and lysosomes (Krause et al., 1994; Steinhardt et al., 1994; Bement et al., 1999; Detrait et al., 2000; Rao et al., 2004; Andrews, 2005; Andrews and Chakrabarti, 2005). From the functional effects of synaptotagmin fragments (Rao et al., 2004; Andrews, 2005; Andrews and Chakrabarti, 2005) and from knockdown studies (Jaiswal et al., 2004), synaptotagmin VII has been proposed to be the Ca sensor in the cell wound response. Dysferlins are another group of Ca-binding proteins with C2 domains that are being considered for a role in cell membrane repair responses, in particular in muscle (Bansal and Campbell, 2004; Washington and Ward, 2006).

In this article, we extend the analysis of Ca-induced membrane fusion in fibroblasts with baby hamster kidney (BHK) cells, using cardiac Na/Ca exchangers to activate a large Ca influx and to manipulate cytoplasmic Ca. For multiple reasons, it appeared important to us to characterize the function of Ca-dependent phospholipases, especially PLCs in the protocols that evoke membrane fusion in fibroblasts. First, phosphatidylinositol 4,5-bisphosphate ($PI(4,5)P_2$), the substrate of PLCs, can bind to and modulate the function of synaptotagmins (Tucker et al., 2003; Bai et al., 2004) and an associated protein, CAPS (Grishanin et al., 2004), which control membrane fusion in the active zones of neurons (Geppert et al., 1994). In addition, there appear to be requirements for $PI(4,5)P_2$ in one or more processes leading up to membrane fusion (Milosevic et al., 2005). Second, diacylglycerol (DAG), the lipid product of PLC activity, can modulate proteins involved in membrane fusion, in particular the munc proteins (Madison et al., 2005; Speight and Silverman, 2005; Latham and Meunier, 2006), and a DAG-dependent PKC can evidently facilitate the cell wound response (Togo et al., 2003; Steinhardt, 2005). In *Xenopus* oocytes, the Ca-dependent exocytosis of cortical granules upon fertilization appears to be initiated by the activation of PKCs by DAG (Gundersen et al., 2002). Both DAGs and phorbol esters can mimic Ca in activating fusion in oocytes, and activation of the Ca-independent PKC-η is implicated to be important (Gundersen et al., 2002). Thus, it is possible that in the oocyte a PLC is the actual Ca sensor for this type of fusion response. In yeast, a novel PLC activity has been suggested to play an important role in homotypic vacuole fusion with DAG serving potentially as a second messenger that facilitates fusion (Mayer et al., 2000; Jun et al., 2004). Finally, it is noteworthy that phospholipases appear to have a fusion-promoting (fusogenic) influence in multiple membrane fusion processes (Harrison and Roldan, 1990; Haslam and Coorssen, 1993; Goni and Alonso, 2000; Choi et al., 2002; Brown et al., 2003; Choi et al., 2006). As described in this article, Ca influx indeed strongly activates PLCs in BHK cells in the same Ca range and on the same time scale in which membrane fusion occurs. In addition, we identify another pronounced membrane change. Extracellular binding of multiple cationic agents suggests that the extracellular cell surface rapidly becomes anionic during and after membrane fusion. We describe a wide range of experiments to address the possible roles of these changes in membrane fusion, and the results suggest that membrane fusion and phospholipid changes are independent processes that are triggered independently by large cytoplasmic Ca transients.

MATERIALS AND METHODS

Cell Lines and Transfections

BHK cells expressing NCX1 (Linck et al., 1998) with and without expression of hM1 receptors were maintained as previously described (Yaradanakul et al., 2007). BHK cells were grown in Dulbecco's modified minimum essential medium (DMEM) supplemented with 10% FBS with periodic selection by 2.5 mg/ml methotrexate for NCX1 and continuous selection with 200 μg hygromycin for hM1 receptors. Lipofectamine 2000 was used for DNA transfections following the manufacturer's protocols. Cells were harvested with 0.25% trypsin and kept at 35°C for 20 min in culture medium before experimentation.

Patch Clamp

Patch clamp and capacitance recording were performed as described previously (Yaradanakul et al., 2007). In brief, giga seals were established with 4–6 μm inner diameter pipette tips that were coated with dental wax before cutting and polishing to reduce capacitance. The majority of capacitance recordings were performed with our own software, described in an accompanying article (Wang and Hilgemann, 2008). Sinusoidal voltage oscillation (20 mV, 0.5–2 kHz) was usually employed when input resistances were <2 MΩ, and square wave oscillation (20 mV, 0.5 kHz) was usually employed when input resistances were 1 MΩ or higher. In the former case, the optimal phase angle was selected digitally via small changes of the optimal capacitance compensation parameters. In the latter case, single exponentials were fit to the falling phase of current transients, and input resistance, cell conductance, and cell capacitance were calculated online. As described in the accompanying article, the routines were validated by simulating typical cell electrical properties with the perturbation

patterns employed, whereby cell parameters and parameter changes could be retrieved with an accuracy of about 99.9%. A few recordings employed phase-lock amplifiers, as described previously (Yaradanakul et al., 2007), and we detected no qualitative or quantitative differences between capactiance recordings performed with the two methods.

For experiments without imaging, the voltage-clamped cells were moved rapidly between four parallel solution streams maintained at 35°C. For experiments with simultaneous confocal imaging, a commercial recording chamber (RC-26; Warner Instruments) was employed in conjunction with a Nikon TE2000-U microscope, and for extracellular solution changes four solution lines with on/off switches were merged to a single temperature-controlled outlet.

Solutions, Chemicals, and Constructs

The standard extracellular solution for maximal outward Na/Ca exchange current contained (in mM) 110 NMG, 20 TEA-OH, 15 HEPES, 3 $MgCl_2$, and 0.5 EGTA, set to pH 7.0 with aspartate, with activation of current by substituting 2 $MgCl_2$ for 2 $CaCl_2$. The standard cytoplasmic solution contained (in mM) 80 NMG, 40 NaOH, 20 TEA-OH, 15 HEPES, 0.5 EGTA, 0.25 $CaCl_2$, 0.5 $MgCl_2$, 1.6 MgATP, 0.4 TRIS-ATP, and 0.2 MgGTP, set to pH 7.0 with aspartate. For Figs. 3–5, 80 mM NMG was replaced in both solutions with 80 mM LiOH. In Fig. 3, 40 mM LiOH was replaced with 40 NaOH in the extracellular solution used to activate exchange current. In the experiments for Figs. 6 and 7, the cytoplasmic solution contained (in mM) 60 NaOH, 30 KOH, 30 TEA-OH, 0.5 $MgCl_2$, 0.5 EGTA, 0.25 $CaCl_2$, 30 HEPES and set to pH 6.9 with aspartate. For experiments with inward exchange current in Fig. 13 C, the extracellular solution contained (in mM) 120 NaOH (or LiOH), 1.5 EGTA, 26 TEA-OH, 20 HEPES, and 1 $MgCl_2$, set to pH 7.0 with aspartic acid. The cytoplasmic solution contained (in mM) 120 LiOH, 20 TEA-OH, 1 $MgCl_2$, 3.0 EGTA, $CaCl_2$ to achieve the desired free Ca, 15 HEPES, 2 ATP, and 0.2 GTP, set to pH 6.9 with aspartic acid. Rhodamine-conjugated hepta-lysine (rhodamine-KKKKKKK-amide; K7-Rhod) was prepared by Multiple Peptide Systems (NeoMPS, Inc.). Annexin-V Alexa Fluor 488 (#A13201) conjugate was from Invitrogen and was employed at 1:100 dilution. All other chemicals were from Sigma-Aldrich and were the highest purity available. The PLCδ1PH-GFP fusion protein construct was a gift of Tobias Meyer (Stanford University, Stanford, CA), and the construct for C1A-GFP fusion protein (Oancea et al., 1998) was provided by Mark Shapiro (UT San Antonio).

Imaging

Confocal imaging was as described (Yaradanakul et al., 2007) with a Nikon TE2000-U microscope and a Nikon 60× 1.45 NA oil immersion objective. A 40 mW Spectra Physics 163-CO2 laser was used for 488/514 nm excitation (i.e., for GFP constructs and FM dye); a 1.5 mW Melles Griot cylindrical HeNe Laser was used for 543.5 nm excitation (i.e., for rhodamine constructs). The time lapse images were recorded either at 160 × 160 or 256 × 256 resolution with an ∼400-ms total exposure time. The exposure interval was 3 s in all records presented. Lasers were operated at 1% power with a detector pinhole setting of 60 µm and an average linear gain of 7.00. Fluroescence intensity is quantified in most figures as percent of maximal fluorescence occurring during the recording (%).

Lipid Analysis

Anionic phospholipid mass measurements were performed as previously described (Nasuhoglu et al., 2002a). The total mono- and diacylglycerols were determined via a bacterial DAG kinase that phosphorylates both mono and diglycerides (Preiss et al., 1987). To do so, phospholipids were first extracted, washed, and dried by the same procedures used for other mass determinations. They were then dissolved in 50 µl of a solution containing 0.3 mM tetradecylsulfate and 0.6% Triton X-100. An equal amount of DAG kinase reaction buffer (2 mM ATP, 2 mM DTT, 100 mM imidazole, 100 mM NaCl, 25 mM $MgCl_2$, 2 mM EGTA, pH 6.6) was then added to separate samples with and without 10 µg/ml DAG kinase (Calbiochem, #266726). The aliquots were reacted to completion in 30 min at 30°C, phospholipids were again extracted and analyzed as previously described (Nasuhoglu et al., 2002a), and the total mono- and diacylglycerol was determined from the increase of glycerol phosphate in HPLC analysis of deacylated phospholipids treated versus not treated with DAG kinase.

Electron Microscopy

The BHK cell preparation for electron microscopy was performed largely as described for other cell types (Sugita et al., 2001). Cells were removed from dishes, as described above, and they were spun down to form loose pellets before fixing in 2% glutaraldehyde with 1% sucrose in 0.1 M sodium cacodylate buffer (pH 7.4) at 37°C for 2 h. The pellets were then carefully separated and rinsed twice in buffer and post-fixed in 0.5% OsO_4, 0.8% K-ferricyanide in the same buffer for 30 min at room temperature. After rinsing with distilled water, specimen were stained in bloc with 2% aqueous uranyl acetate for 15 min, dehydrated in ethanol and embedded in Poly/bed 812 for 24 h. Thin sections (65 nm) were post-stained with uranyl acetate and lead citrate, and they were viewed with an FEI Tecnai G2 Spirit Biotwin transmission electron microscope.

RESULTS

BHK Cell Response to Maximal NCX1-mediated Ca Influx

Fig. 1 presents a typical electrophysiological recording from an NCX1-expressing BHK cell during repeated brief activation of the maximal outward exchange current when the cytoplasm was weakly Ca buffered. Whole-cell current, capacitance, and conductance are monitored as described in Materials and methods with a 20-mV sinusoidal voltage oscillation at 500 Hz. The cytoplasmic solution contains 2 mM ATP, 0.2 mM GTP, 40 mM Na, and 0.5 mM EGTA with 0.25 mM Ca (0.4 µM free Ca), and the extracellular solution is Na free. The outward current is activated by switching from an extracellular solution with 0.5 mM EGTA and no Ca to one with 2 mM Ca (i.e., 1.5 mM free Ca; see Materials and methods for further details). Panel A shows the entire experimental records over 6 min in which the exchange current was activated and deactivated four times. Panel B shows the records during each activation cycle at higher time resolution, together with the calculated capacitance derivative (*dCap/dt*).

The peak outward current is 1.23 nA in the first response, and the average current for the initial 1-s activation time is 0.85 nA. We estimated cell volume to be 10 pL, the cell being nearly round under these conditions with a maximal diameter of 28 µm. Thus, the initial rate of Ca influx, assuming 3Na/1Ca exchange, corresponds to 1.2 mmol per liter cell volume per second, and the total Ca influx is estimated to be >1 mmol per liter cell volume during the 1-s application of extracellular Ca.

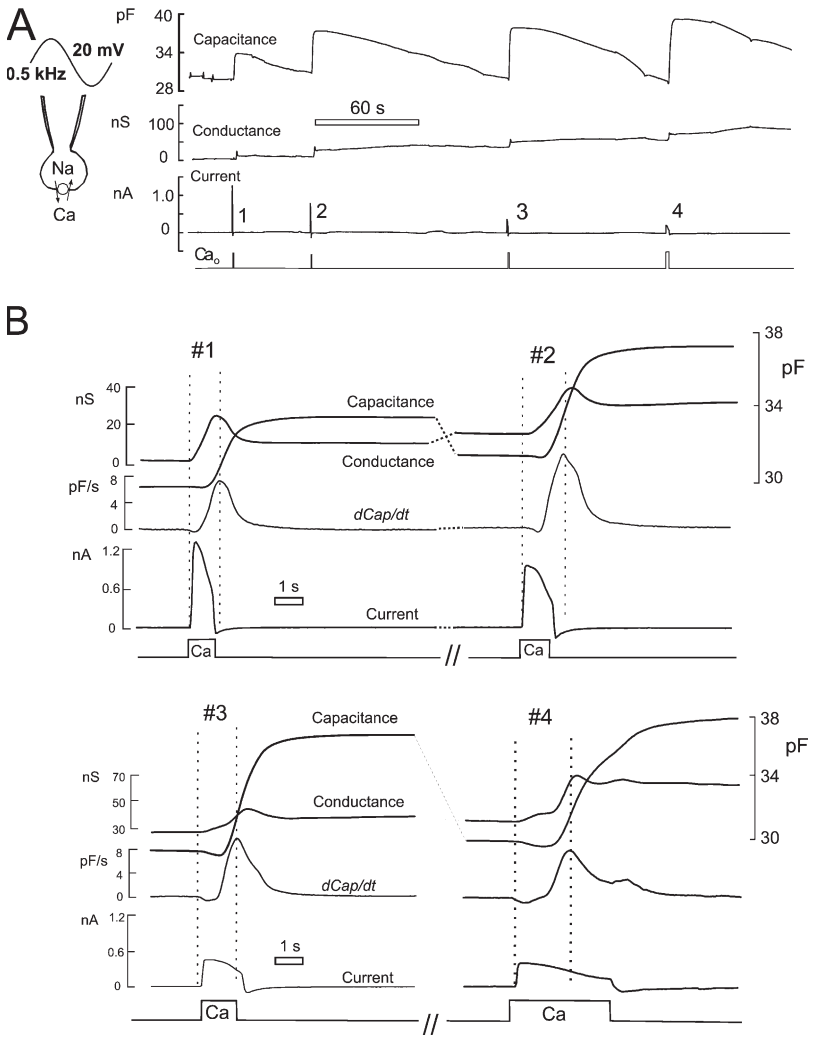

Figure 1. Typical records of membrane capacitance, conductance, and current from BHK cells consitutively expressing the cardiac Na/Ca exchanger (NCX1). Cell parameters are monitored via 20-mV sinusoidal membrane voltage perturbation at 0.5 kHz. Input resistance ≈ 1 MΩ. Cytoplasmic solution contains 40 mM Na and 0.5 mM EGTA with 0.25 mM Ca (free Ca, 0.4 μM). Exchange current was activated four times for increasing durations of 1–6 s by applying and removing 2 mM extracellular Ca, as indicated below the records. (A) Complete signal records. (B) Expanded signal records for the time periods during and immediately after activation of exchange current. *dCap/dt* is the first derivative of capacitance. Two vertical dotted lines in each activation cycle mark the time when current was activated and the time at which the maximal rate of rise of capacitance occurred. Note that the rise of capacitance is preceded by a small negative capacitance phase. The time from current activation to peak rate of rise of capacitance increases as the peak exchange current decreases in this sequence.

Membrane capacitance starts to rise and achieves a maximal rate of rise at roughly the time point of complete exchange current deactivation. The rise of capacitance occurred typically with a delay of at least 0.1 s. The rise was often preceded by a decline, amounting to a few percent of the final rise (see negative derivative signal). The initial cell capacitance was 30.6 pF in this experiment, the maximal rate of rise of capacitance was 7.5 pF/s, and the total increase of capacitance at the first Ca pulse amounted to 4 pF (i.e., 13% of the initial cell capacitance). The cell resistance was 0.3 GΩ (3 nS) before activating exchange current.

During Ca influx, the cell conductance increases by 20 nS within 700 ms and then decreases partially toward baseline. The irreversible component of this increase probably reflects a decrease of seal resistance. The transient part of the response may in part reflect exchange current activity, but several arguments suggest that it reflects mostly conductive properties of fusion pores (Lindau and Alvarez de Toledo, 2003; Neef et al., 2007). First, the transient conductance changes do not track exchange current. Conductance rather rises slowly after exchange current has been completely activated. Second, the outward NCX1 current under the conditions of these experiments (i.e., with 120 mM extracellular NMG and no other extracellular monovalent cations) is nearly voltage independent (Matsuoka and Hilgemann, 1992; Matsuoka and Hilgemann, 1994) and therefore is not expected to contribute substantial conductance changes. Third, the slow rise of conductance correlates roughly in time with the rate of rise of capacitance (i.e., *dCap/dt*), and the peaks of these signals occur at approximately the same time, as denoted by a second dotted vertical line in each response.

The peak exchange current typically decreased by at least 40% from one Ca pulse to the next with Ca pulse durations of 1–5 s. Also evident in these records, the rise of capacitance typically occurred with a longer delay at the second and later responses when the exchange current was decreased. Nevertheless, the second increase of capacitance was typically larger and occurred with a higher maximal rate than during the first response. This is consistent with reports that the cell wound response shows facilitation when induced multiple times (Togo et al., 2003).

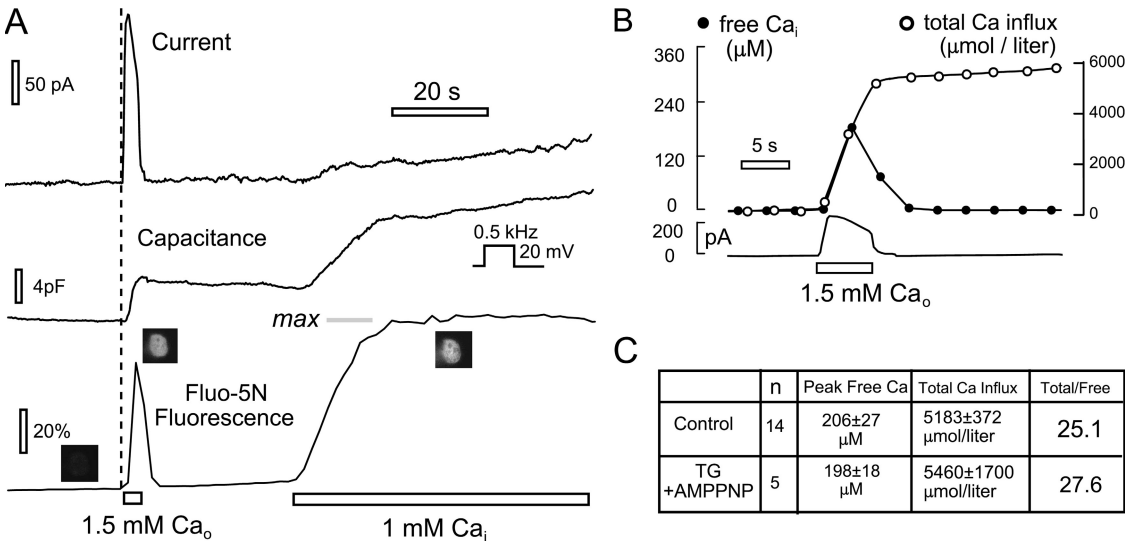

	n	Peak Free Ca	Total Ca Influx	Total/Free
Control	14	206±27 μM	5183±372 μmol/liter	25.1
TG +AMPPNP	5	198±18 μM	5460±1700 μmol/liter	27.6

Figure 2. Measurement of cytoplasmic free Ca changes during activation of outward Na/Ca exchange currents in BHK cells. The pipette solution contains 0.5 mM EGTA and 0.25 mM Ca (i.e., 0.4 μM free Ca) with 3 μM Fluo 5N (K_d, 90 μM). Here, and in all figures, Ca concentrations given indicate the free Ca concentration. (A) Typical fluorescence and current records. When 2 mM Ca is applied for 4 s, current rises rapidly to a peak of 175 pA and decays to baseline within <1 s when Ca is removed. Peak fluorescence occurs at 3 s and begins to decay rapidly before current is deactivated. Upon perfusion of the pipette with 1 mM additional Ca, fluorescence rises to a steady "maximal" level with a time constant of ∼20 s. (B) Free and total Ca are calculated from the fluorescence and current records as described in the text. Peak free Ca is estimated to be 0.20 mM at a time point when total Ca influx amounts to 3.0 mmol/liter cell volume. (C) Peak free and total Ca influx values obtained 14 control cells and 5 cells perfused with 2 μM thapsigargin and 2 mM AMP-PNP to block Ca pumping. Results are not significantly different.

As in most experiments, the same magnitude of capacitance increase was achieved at the third and fourth Ca pulses when the Ca pulse period was increased to compensate for the decreased exchange current.

We stress that both the magnitudes of capacitance increase and the extent to which capacitance signals reversed to baseline were somewhat variable and showed statistically highly significant dependence on cell batch and growth conditions. The average increase of capacitance was found to vary by up to fivefold between cell batches with similar basal capacitance and exchange current density. For example, we verified in two datasets that removal of serum from cells for 24 h caused a highly significant decrease of the capacitance response by >50%, while the exchange current density was unchanged. In ∼50% of cell batches, cell capacitance did not reverse completely, as occurs in Fig. 1, and in ∼25% of cases the cell capacitance decreased to values lower than the initial cell capacitance before activating Ca influx. Rarely, reversal amounted to only a small fraction of the initial capacitance increase, and capacitance increments were then very small at the second to fourth Ca pulses. Finally, we mention that capacitance responses in CHO and HEK293 cells were typically smaller than those of BHK cells when equivalent NCX1 expression was achieved by transient or stable expression methods. Responses in CHO cells seldom exceeded 40% of basal cell capacitance, and responses in HEK293 cells were usually close to 15%.

Current and Ca Dependencies of Capacitance Responses

Using the protocol described in Fig. 1, we proceeded to analyze the exchange current and Ca dependencies of the capacitance responses. As evident in Fig. 1 B, capacitance increases smoothly during the same time period in which exchange current is deactivated by removing extracellular Ca. This observation indicates that Na/Ca exchangers do not generate a local Ca signal that is critical for this type of membrane fusion. To determine the mean free Ca concentrations occurring in cells, we employed the low affinity Ca indicator dye fluo-5N (Invitrogen) at a concentration of 3 μM in the pipette solution. Fig. 2 A shows a typical fluorescence record obtained during NCX1 activation under the same conditions as Fig. 1 (0.5 mM EGTA with 0.25 mM total Ca, 0.4 μM free Ca). After recording background fluorescence for 1.5 min, the cell was exposed to 2 mM extracellular Ca for 3 s, as is usual with substitution for 2 mM Mg, fluorescence signals were allowed to dissipate for 30 s. Then, the same cytoplasmic solution was perfused into the cell with the dye saturated by 1 mM free Ca (i.e., 1.5 mM total Ca with 0.5 mM EGTA) to determine the maximal Ca response of the dye in the cell. Peak free Ca induced by Ca influx was then estimated assuming a K_d for Ca of 90 μM with free Ca calculated as $K_d/(F_{max}/F-1)$, where F_{max} is the cell fluorescence with Ca-saturated fluorophore and F is the peak fluorescence obtained in response to activating Ca influx.

Fig. 2 B shows our calculation of total Ca influx (i.e., the integral of the exchange current related to the estimated

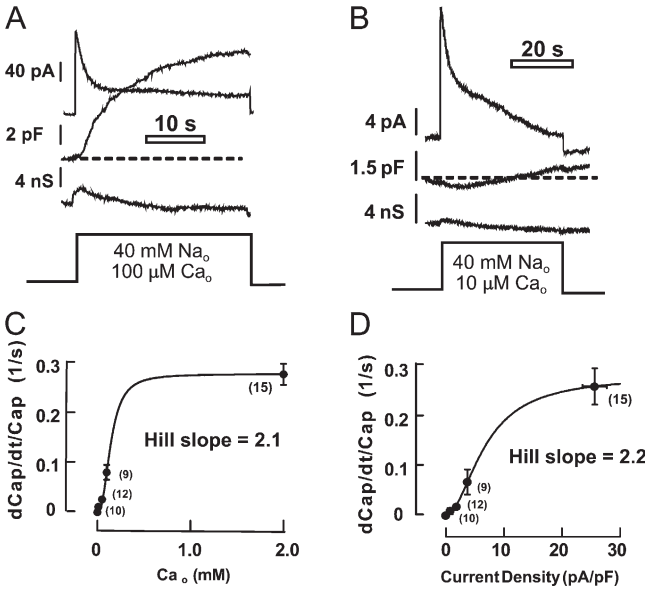

Figure 3. Dependence of BHK cell capacitance responses on the extracellular Ca concentration and exchange current density (0 mV, 35°C). (A) Typical current, capacitance, and conductance records during application of 0.1 mM free Ca together with 40 mM Na, thereby limiting the maximal free cytoplasmic Ca concentration to 0.1 mM. (B) Typical current, capacitance, and conductance records during application of 10 μM free Ca together with 40 mM Na, thereby limiting the maximal free cytoplasmic Ca concentration to 10 μM. (C) Maximal rate of capacitance increase as fractional increase of total cell capacitance per second (dCap/dt/Cap) in dependence on the applied extracellular free Ca. (D) Maximal fractional rate of capacitance rise in dependence on peak exchange current density.

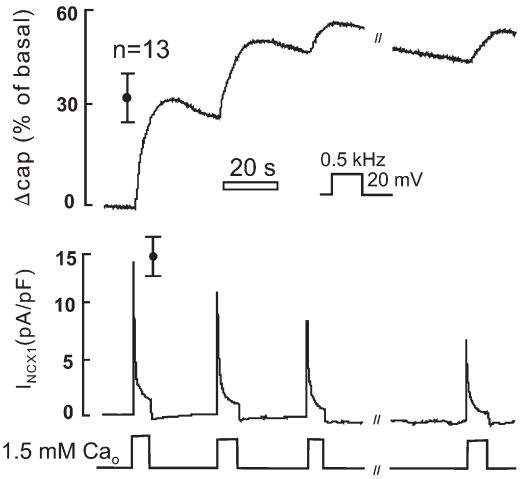

Figure 4. Capacitance and current record of a BHK cell expressing NCX1 in perforated patch whole cell configuration. Same solutions as previous figures with 40 μM β-escin in the pipette solution and capacitance recording via square wave perturbation. Error bars represent the results of 13 similar experiments.

cell volume) and the free Ca from the calibration just described. In this experiment, peak free Ca is 170 μM and total Ca influx is estimated to amount to 6 mmol/liter cell volume. At the peak of the Ca transient, the ratio of total to free Ca is estimated to be 25. As shown in Fig. 2 C, the average peak free Ca for 14 cells was 206 μM, and the average total Ca influx amounted to 5,183 μmol/liter cell volume. A major concern about this dye calibration method is whether the maximal fluorescence really reflects fluorescence of the saturated dye or whether free Ca might still be significantly controlled by cellular Ca pumps. Therefore, we performed a series of experiments in which the cytoplasmic solution contained thapsigargin (2 μM), as well as adenosine 5′-(β,γ-imido) triphosphoate (AMP-PNP) (2 mM), to ensure that Ca pumps were inactive. As evidence of efficacious pump inhibition, the time from peak to 50% decay of the Ca transients was increased by 2.4-fold in the treated cells (unpublished data). As shown in Fig. 2 C, inhibition of Ca pumps did not affect exchange currents (i.e., the calculated total Ca influx is unchanged), and the calculated peak free Ca was unchanged. Accordingly, we conclude that the free Ca is accurately determined by the protocol of Fig. 2 A.

From experiments in which we employed BHK cell lines with different NCX1 current densities, our impression was that the rate and extent of capacitance increase were nearly proportional to the current density. As described in Fig. 3, we analyzed quantitatively the relationships between peak current density and capacitance changes by varying extracellular Ca. By performing these experiments in the presence of 40 mM Na on both membrane sides, at 0 mV, the maximal free cytoplasmic Ca is thermodynamically limited to not exceed the free Ca applied to the extracellular side. Fig. 3 (A and B) shows representative results for applying 100 and 10 μM free Ca together with 40 mM extracellular Na. We quantified the rate of rise of capacitance as the fractional increase of cell capacitance per second (*dCap/dt*/Cap, i.e., *dCap/dt* divided by the basal cell capacitance). Fig. 3 C presents the dependence of capacitance change on the extracellular Ca concentrations employed (i.e., the maximal possible cytoplasmic free Ca), and Fig. 3 D presents the dependence on the peak current density. The maximal fractional rate of rise of capacitance is ~0.3 per second (i.e., 30% per second). In both plots, the rate of rise of capacitance shows a sigmoidal dependence on current with a Hill coefficient of ~2. Half-saturation occurs at 140 μM free extracellular Ca and 8 pA/pF, respectively. From these results and knowledge of the peak Ca/peak current density relationship from Fig. 2, we conclude that a free Ca concentration >10 μM is required to achieve 10% of the maximal fusion rate, and that a concentration >100 μM is required to achieve the half-maximal fusion rate. We mention that the capacitance delay, defined as the time from activation of current to the time at which capacitance crossed the zero line (see Fig. 3 B), decreased with increasing

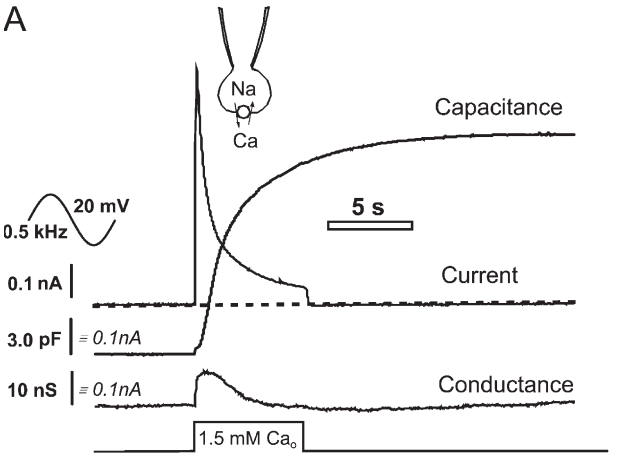

Figure 5. Effects of nonhydrolyzable ATP analogue and protein phosphatase inhibitors on the BHK cell capacitance response and exchange current rundown. (A) Capacitance, conductance, and current records from a BHK cell perfused with 2 mM AMP-PNP for 4 min before activating exchange current. (B) Capacitance changes and peak exchange current densities for control cells, cells perfused with 2 mM AMP-PNP, cells perfused with 2 mM AMP-PNP, and with 5 μM cyclosporin for 4 min before activating exchange current, and cells perfused with AMP-PNP with 9 mM pyrophosphate and 4 mM fluoride.

current density in an almost linear fashion (unpublished data).

Other Experimental Factors

Next, we tested how the magnitude and speed of responses were influenced by the speed of Ca transients and several other potentially important experimental factors. Ca influx rates achieved with the Ca ionophore, A23187, were in general not adequate to cause large capacitance responses. To achieve the highest possible Ca influx rates with A23187, cells were incubated with high concentrations of ionophore (10 μM) in the absence of extracellular Ca, and then 1 mM extracellular Ca was applied as in experiments with NCX1. Capacitance responses remained rather small and occurred with much larger time constants (20–50 s) than for activation of NCX1 outward current. Similarly, capacitance responses to pipette perfusion of cytoplasmic solutions with high Ca (e.g., 1.5 mM Ca with 0.5 mM EGTA, as in Fig. 2 A) were much slower than for exchange current activation, and responses were often blunted or negative if pipette perfusion was not rapid. Another factor that raised concern in early experiments was our use of large tip diameters to facilitate voltage clamp and pipette perfusion of the cytoplasm. In this regard, we can report that results were very similar when conventional patch pipettes were employed. As shown in Fig. 4, we also checked whether results might be dependent on dialysis of the cytoplasm. To do so, we performed similar experiments with a perforated patch clamp technique, specifically the β-escin method (Fan and Palade, 1998) that allows fast cell dialysis with a molecular weight cutoff of 5–10 kD. Using a concentration of 40 μM detergent, perfused into the pipette tip with the standard cytoplasmic solution, we monitored the establishment of voltage clamp using square wave voltage oscillation. In most cells, access resistances decreased to <5 MΩ, and square wave voltage oscillation allowed accurate capacitance analysis. Fig. 4 shows a typical experiment together with composite results for 13 experiments. In brief, capacitance changes were similar in magnitude to results presented above, the average increase being 28% in this series. The rates of capacitance increase and subsequent reversal are both somewhat lower than averages for several batches of BHK cells with normal whole-cell patch clamp. Peak exchange currents decreased from one Ca influx episode to the next roughly to the same extent as in the routine whole-cell results.

Metabolic Dependence of Membrane Fusion

We next address the question of whether metabolic processes significantly control and/or modulate this type of membrane fusion, ATP-dependent processes in general, and protein phosphorylation in particular. In the experiments described in Fig. 5, ATP and GTP were both replaced in the cytoplasmic solution with a nonhydrolyzable ATP analogue, AMP-PNP (2 mM). Fig. 5 A shows a typical fusion response after cytoplasmic perfusion with AMP-PNP for 4 min. The capacitance response is still large, and the maximal rate of capacitance change, 9 pF/s (14% per second), occurs as usual ~0.5 s after starting Ca influx. The final increase of capacitance is just 40% of the initial cell capacitance. Thus, long-term ATP removal clearly does not block cell capacitance responses. Nevertheless, analysis of multiple responses reveals that the extent of the capacitance responses is significantly blunted by the ATP analogue. As shown in the first two data bars of Fig. 5 B, the response magnitudes were reduced by 55%. To test whether this decrease might require a protein phosphatase activity, we perfused cells from the same cell batch with 5 μM cyclosporin to test for a role of calcineurin and with 4 mM fluoride and 9 mM pyrophosphate to inhibit phosphatases nonselectively. As shown further in Fig. 5 B, the capacitance responses were not significantly restored in AMP-PNP solutions by these interventions. The peak NCX1 current was significantly increased by fluoride and pyrophosphate. We stress however that Mg will be

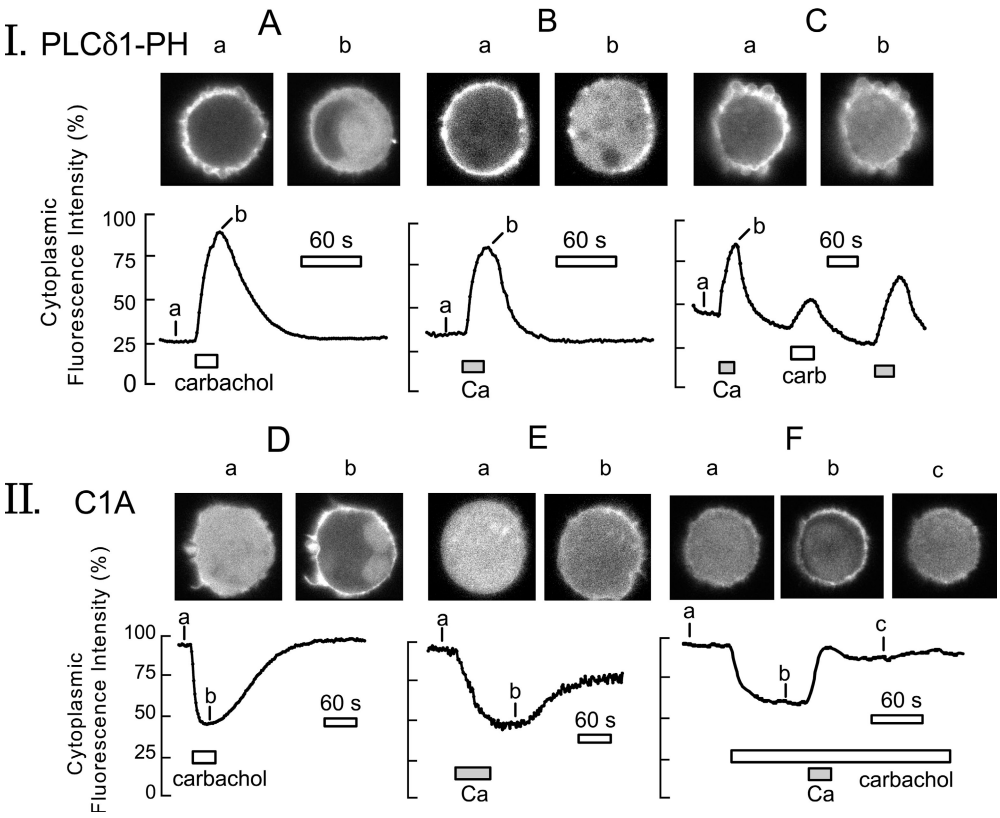

Figure 6. PLC activation monitored via PLCδ1PH-GFP (panel I) and C1-GFP (panel II) protein fusions in BHK cells voltage clamped to 0 mV via large-diameter pipette tips. The continuous records give the average fluorescence in a central region of the cytoplasm. As evident in micrographs, shown above the cells, the large-diameter tips promote bleb formation. (Panel I, A) The PLCδ1PH-GFP domain, initially localized mostly to the surface membrane, rapidly translocates to the cytoplasm during carbachol (0.3 mM) application for 20 s. When agonist is removed, PH domains return to the cell membrane with a time constant of ~32 s. (B) Similar PH domain responses recorded when cells are loaded with high Na (40 mM) and Ca influx via NCX1 is activated for 12 s by applying and removing 2 mM extracellular Ca. (C) Comparison of PH domain signals in a cell activated first by Ca influx, then by carbachol, and finally again by Ca. (Panel II, D) The C1 domain is initially cytoplasmic and then rapidly translocates to the membrane during carbachol (0.3 mM) application for 20 s. (E) Slower and smaller C1 domain response, typically obtained during activation of outward NCX1 current. (F) Typical C1 domain cytosolic fluorescence changes when carbachol (0.3 mM) is applied continuously and Ca (2 mM) is then applied for 15 s together with carbachol, followed by washout. C1-GFP domains dissociate rapidly from the plasma membrane during Ca influx and accumulate diffusely in the cytoplasm.

chelated in this protocol. From our own experience as well as the literature (DiPolo et al., 2000; Wei et al., 2002), cytoplasmic Mg chelation significantly stimulates the reverse exchange operation.

Ca-activated PI(4,5)P_2 Cleavage

As outlined in the Introduction, recent studies suggest that phosphoinositide metabolism can modulate some membrane fusion processes. From previous studies (Rhee, 2001; Nasuhoglu et al., 2002b) the free Ca concentrations occurring in our experiments can be expected to cause activation of PLCs and PI(4,5)P_2 depletion. Thus, it seemed important to analyze in detail PI(4,5)P_2 breakdown during these protocols in BHK cells in relation to the capacitance responses. Figs. 6–9 present the major electrophysiological, optical, and biochemical results from these experiments.

First, we compared PI(4,5)P_2 breakdown in BHK cells in response to activation of a G protein–coupled receptor (GPCR) that activated PLCs and a rise of cytoplasmic Ca via NCX1. To do so, we expressed PLCδ1PH-GFP fusion protein together with M1 receptors (Selyanko et al., 2000) in BHK cells expressing NCX1 constitutively. Fig. 6, panel I, shows typical fluorescence changes of BHK cells expressing PH domains in response to maximal M1 receptor activation with 0.3 mM carbachol (Fig. 6 A), in response to maximal outward exchange current (B), and then sequentially to Ca and carbachol in the same cell (C). The fluorescence curves give the average cytoplasmic fluorescence of the voltage-clamped BHK cells, perfused internally with 0.5 mM EGTA and 60 mM Na at 35°C with corresponding cell micrographs given above the records. Note that cells are nearly round under the conditions of the experiments, and that some cells form large blebs after opening with large-diameter pipette tips, even before activating receptors or Ca influx.

In response to carbachol (Fig. 6 A), cytoplasmic fluorescence rises by fourfold within 20 s as PLCδ1PH-GFP domains are lost from the cell surface. Upon removal of carbachol, the amount of cytoplasmic fluroescence begins to decrease within 5 s and returns to baseline in a nearly exponential fashion with a best-fit time constant of 32 s. In response to activation of outward NCX1 current for 12 s (Fig. 6 B), PLCδ1PH-GFP domain responses of similar magnitude and kinetics are recorded. As shown in Fig. 6 C, the magnitudes of responses to

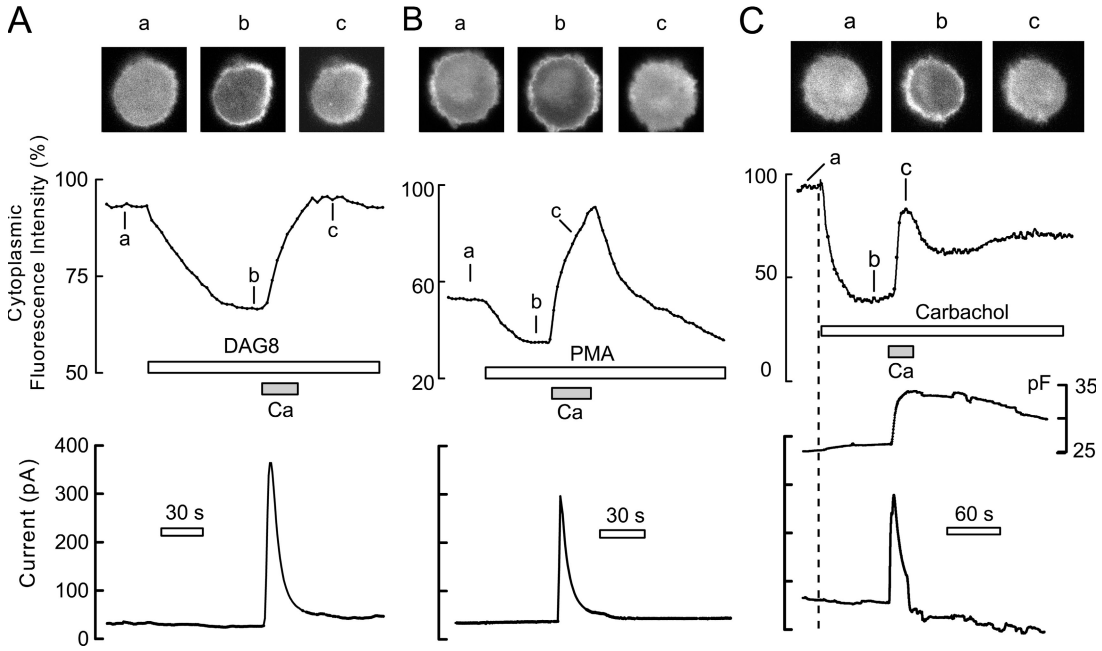

Figure 7. Translocation of C1-GFP domains to the surface membrane of BHK cells by short-chain DAG8 (A), phorbol ester (B), and carbachol (C), followed by redistribution to the cytoplasm in all three cases by activation of Ca influx (i.e., outward NCX1 current). (A) Application of 20 µM C8 diacylglycerol brings the majority of C1 domain to the surface membrane with a time constant of ~45 s. Upon activating reverse exchange current, domains return quantitatively to the cytoplasm with a time constant of ~35 s. (B) Application of 0.2 µM phorbol ester (PMA) brings C1 domains to the cell surface with a time constant of ~30 s. During activation of exchange current, C1 domains reach a substantially higher concentration in the cytoplasm than in the basal state with a time constant of ~30 s, and C1 domains begin to move back to membrane immediately upon terminating Ca influx. (C) C1-GFP domain records together with cell capacitance and membrane current in a BHK cell expressing NCX1 and hM1 receptors. With application of carbachol (0.3 mM) cytoplasmic fluorescence decreases by 60% with a time constant of ~20 s, and cell capacitance increases modestly. Upon activation of Ca influx, cell capacitance increases by ~8 pF (30%) in less than 10 s, and C1 domains accumulate again in the cytoplasm with time constant of ~10 s. Upon deactivating exchange current, C1-GFP domains move partially back to the surface membrane.

activation of NCX1 were typically at least as large as the responses to carbachol in the same cell, and responses could be repeated multiple times with only little loss of signal magnitude.

From these results, it is clear that Ca influx can activate large PLC responses in BHK cells. To determine more accurately the Ca range over which PLCs become activated, we analyzed PH domain distributions in dependence on the inward exchange current in the presence of different free Ca concentrations in the pipette solution. From previous experiments, it is clear that free cytoplasmic Ca decreases significantly during activation of inward current by extracellular Na, even in the presence of several millimolar EGTA buffering (Yaradanakul et al., 2007). Since the free cytoplasmic Ca cannot exceed the free Ca of the patch pipette solution, protocols with inward current can give a clear indication of the minimum Ca required to activate PLCs in the absence of receptor activation. To summarize briefly results from >20 experiments, removal of extracellular Na to deactivate inward current caused clear PLC activation when cells were perfused with solutions containing free Ca of 20 µM or higher. When cells were opened with free Ca of 8 µM or less, the activation and deactivation of inward exchange currents had no evident effect on the PH domain distribution in cells (unpublished data). Thus, we conclude that free Ca in the range of 10 µM is needed to significantly activate PLCs in the absence of GPCR activation.

Given that high free Ca can strongly activate $PI(4,5)P_2$ breakdown in BHK cells, it may be expected that PLC activity will contribute to NCX1 current rundown in the protocols with massive Ca influx. However, as just described, the PH domains redistribute reversibly in response to both carbachol and Ca changes on a rather fast time scale. By comparison, the suppression of outward exchange current in response to Ca influx episode is very long-lived and often does not reverse at all (Figs. 1 and 4). Thus, $PI(4,5)P_2$ depletion cannot be the sole or even the major mechanism of long-term exchange current inactivation and rundown in the experiments described.

Dual C1A Domain Responses to a Rise of Cytoplasmic Ca

In panel II of Fig. 6, and in Fig. 7, we describe responses of the DAG-binding C1A-GFP fusion proteins (Oancea et al., 1998). Fig. 6 (D and E) shows the usual signals observed for carbachol and NCX1 activation, respectively

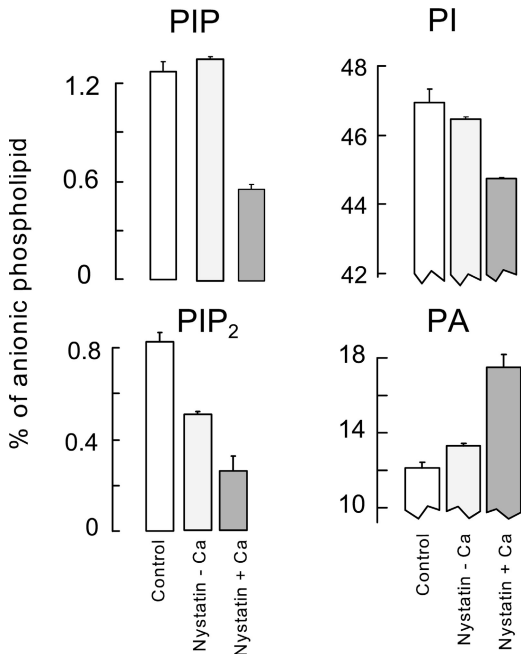

Figure 8. Phosphoinositide and phosphatidate changes in BHK cells in response to Ca influx via NCX1. The bar graphs represent the relative phospholipid concentrations, as percent of total anionic phospholipid, for cells under control conditions (control), cells treated with 25 μM nystatin in the absence of Ca for 10 min (nystatin − Ca), and nystatin-treated cells that were exposed to 4 mM extracellular Ca for 1 min (nystatin + Ca).

(>20 observations), and F illustrates a major complexity encountered. As shown in D and E, the C1 domain appears almost uniformly distributed throughout the cytoplasm in unstimulated, voltage-clamped BHK cells. When M1 receptors are overexpressed, as in all three cells depicted, application of carbachol (0.3 mM) results in the association of these domains with the membrane within 20 s. Upon removal of carbachol, the domains reequilibrate into the cytoplasm with somewhat larger time constants (90 s) than those just described for PH domains. Thus, metabolism of DAG by lipases and kinases may be somewhat slower than resynthesis of $PI(4,5)P_2$ (i.e., phosphorylation of PI and PIP). As apparent in Fig. 6 E, activation of Ca influx by NCX1 causes a qualitatively similar response to that of carbachol, as anticipated, but the extent of the responses and the rate of rise of the responses were consistently less than for carbachol. As shown in Fig. 6 F, the blunted response of C1A domains to Ca elevation reflects a second, strong opposing influence of Ca on the distribution of C1 domains. This opposing influence is vividly revealed when the C1 domains are first brought to the membrane by carbachol, and then extracellular Ca is applied to induce a rise of cytoplasmic Ca in the continued presence of carbachol. As shown in Fig. 6 F, Ca influx in the presence of carbachol results in a rapid return of C1 domain to the cytoplasm whereby a nearly uniform distribution develops with a time constant of just 15 s.

As summarized in Fig. 7, we next tested how Ca influx affects the C1 domain distribution when domains are brought to the surface membrane by applying exogenous C1 domain-binding reagents, specifically short chain diocylglycerol (DAG8, 20 μM) and phorbol ester (PMA, 0.2 μM). As shown in Fig. 7 (A and B), these agents cause a pronounced loss of C1-GFP domain from the cytoplasm and accumulation at the cell surface (a to b). Subsequent activation of NCX1 outward current by a 20–30-s application of extracellular Ca results in complete translocation of C1 domains back to the cytoplasm. In the example shown for PMA (Fig. 7 B) it appears possible that DAG-generating mechanisms are significantly active in the absence of agonist, as there is a substantial overshoot of C1 domain in the cytoplasm upon activating Ca influx. The cytoplasmic redistribution of C1 domains reverses over 2 min when the Ca influx via NCX1 is stopped by removal of extracellular Ca. Fig. 7 C presents in more detail C1 domain responses (i.e., cytosolic C1 domain fluorescence) together with membrane capacitance and current during continuous activation of M1 receptors with a short activation of outward exchange current by extracellular Ca. Carbachol is applied for 100 s before activation of NCX1. During this time, ∼60% of C1 domains move out of the cytoplasm with a time constant of ∼20 s, and cell capacitance increases by ∼1 pF. Activation of NCX1 for 20 s causes an 8-pF increase of capacitance, corresponding to a 30% increase of cell capacitance. Within this same time frame, 80% of C1 domains return to the cytoplasm and exchange current decreases by 75%. As exchange current decreases and is deactivated by removing extracellular Ca, C1 domains are again lost from the cytoplasm partially. However, the C1 domain population in the cytoplasm remains elevated substantially from the nadir achieved during the initial application of carbachol. We conclude from these experiments that the distribution of C1 domains between the cell membrane and cytoplasm is subject to both rapid, short-term effects of raising Ca and longer-term influences.

Phospholipid Changes in Response to Changes of Cytoplasmic Ca

We can suggest four mechanisms by which high cytoplasmic Ca may cause translocation of C1 domains from the cell surface to the cytoplasm, and we attempted to eliminate these one by one in appropriate experiments. First, DAG metabolism may be Ca dependent, a major mechanism being that some DAG kinases are activated by Ca (Jiang et al., 2000a; Luo et al., 2004; Topham, 2006). Second, C1 domains interact not only with DAG but also with negatively charged phospholipids, especially PS (Bittova et al., 2001; Ho et al., 2001), which can bind Ca (Wilschut et al., 1981; Papahadjopoulos et al.,

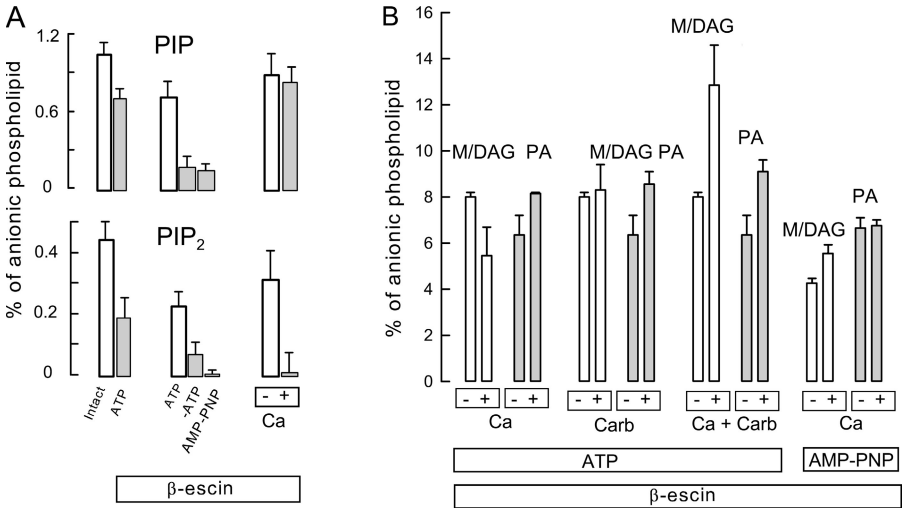

Figure 9. Phosphoinositide, phosphatidate, and total mono/diacylglycerol (M/DAG) levels of permeabilized BHK cells in dependence on ATP, AMP-PNP, and Ca. (A) PIP and PI(4,5)P_2 levels of BHK cells permeabilized with 40 μM β-escin. All results are the average of two to four measurements. Left bars give levels for control cells and permeabilized cells with 2 mM ATP and no Ca (0.5 mM EGTA). The set of three bars in the middle give PIP and PI(4,5)P_2 levels with ATP, without ATP for 5 min, and with 2 mM AMP-PNP for 5 min. The right two bars give phospholipid levels of control cells and cells exposed to 0.4 mM free Ca for 2 min. (B) From left to right, the bar graphs give mono and diacylglycerol (M/DAG) and phosphatidate (PA) levels without and with 0.4 mM free Ca for 1 min (left four bars), without and with 0.3 mM carbachol for 3 min, without and with 0.4 mM free Ca together with 0.3 mM carbachol, and without and with 0.4 mM free Ca for 1 min in the presence of AMP-PNP and no ATP (right four bars).

1990) and thereby might cause release of C1 domains from the membrane. Third, DAG might be generated by PLCs on internal membranes by multiple Ca-dependent mechanisms, thereby favoring translocation of C1 domains to the cytoplasm. And fourth, DAG might translocate to the outside of the cell during membrane fusion, assuming that phospholipid mixing between bilayers occurs during fusion, thereby decreasing DAG on the inner membrane leaflette and releasing C1 domain back to the cytoplasm. In this light, we performed both fluorescence and biochemical studies to determine how a rise of cytoplasmic Ca affects phosphoinositides, DAG, and phosphatidic acid, and how those effects depend on cytoplasmic ATP.

Three types of experiments address whether Ca-activated DAG kinase activity might play a role in the C1 domains translocation to the cytoplasm in response to Ca influx. The first type of evidence is represented by the PMA experiment in Fig. 7. PMA is not phosphorylated by DAG kinases, and yet activation of Ca influx causes C1 domains to move to the cytoplasm after being brought to the cell surface by PMA. In this response, DAG kinase activity at the cell membrane cannot be the cause of the C1 domain movement. Second, we tested for inhibition of C1 translocation by the two available DAG kinase inhibitors at concentrations recommended for strong inhibition (DAG kinase inhibitors I and II [Calbiochem]; R59022 and R59949, each at 10 μM). We found no inhibition of the C1 translocation by either of these agents (unpublished data; two observations each) upon activating Ca influx. These results alone are not conclusive because not all DAG kinases are inhibited by these agents (Jiang et al., 2000b), and we report in this same connection that a substantial rise of phosphatidic acid that occurs in parallel with loss of phosphatidylinositol during M1 receptor activation (Li et al., 2005) was unaffected by the DAG kinase inhibitor, R59022, at a concentration of 20 μM. Third, we performed the protocols of Fig. 7 with 2 mM AMP-PNP and no ATP in the pipette solution, and the C1 domain still translocated rapidly to the cytoplasm when Ca influx was activated (two observations). On this basis, the activation of DAG kinase activity at the cytoplasmic cell surface by a rise of cytoplasmic Ca seems eliminated as a cause of the C1 domain translocation.

As described in Figs. 8 and 9, we measured phospholipid changes in response to increasing cytoplasmic Ca in two different approaches using BHK cells. In the first approach, we used NCX1 to mediate a large Ca influx. To do so, the ionophore, nystatin (25 μM), was applied to load cells with Na in Ca-free PBS (130 mM NaCl, 20 mM HEPES, 15 mM glucose, pH 7.4) for 10 min. Thereafter, 4 mM Ca was added to the extracellular medium for 1 min without addition of Na (130 mM TEA-Cl). Anionic phospholipids were then determined as described, and the relative mass of the four phospholipids of most interest (PIP, PI(4,5)P_2, PI, and PA) are shown in Fig. 8. Calibrations are given as percent of total anionic phospholipid, whereby the majority of anionic phospholipid is PS and cardiolipin. The nystatin treatment resulted in a 30% reduction of PI(4,5)P_2 in the absence of Ca, and there was little or no change of other phospholipids. The Ca addition caused PIP to fall by 70% and PI(4,5)P_2 to fall by 50%, as expected for PLC activation. During the

same 1 min, PI fell from 46.3 to 44.3% of total anionic phospholipid, while PA increased from 12.8 to 17.4% of total phospholipid. As with receptor activation, the fact that PI mass decreases and PA mass increases by similar amounts, more than threefold greater than changes of PIP and $PI(4,5)P_2$, suggests that there is a substantial flux of phospholipid from PI to PIP to $PI(4,5)P_2$ to DAG and finally to PA in this protocol. In summary, these results for cytoplasmic Ca elevation are qualitatively very similar to, but quantitatively less drastic, than published results for M1 receptor activation in cells with constitutive receptor expression (Li et al., 2005).

In another approach, we established a BHK model with the surface membrane permeabilized by β-escin (40 μM). As already noted, this concentration of β-escin generates pores in most cells with a permeation cutoff of 5–10 kD (Fan and Palade, 1998). Therefore, we used this model to analyze the dependencies of anionic phospholipids and the total di- and monoacylglycerol on Ca, both in the presence and absence of ATP. An extracellular solution containing isotonic KCl (140 mM) with 2 mM ATP, 0.2 μM free Ca (1 mM EGTA with 0.2 mM Ca), and 2 mM $MgCl_2$ was employed. As demonstrated in Fig. 9 A, phosphoinositide levels become highly dependent on the presence of nucleotides in the extracellular medium in this model, thereby demonstrating that the surface membrane is highly permeable to solutes. PIP and $PI(4,5)P_2$ levels of permeabilized cells were 30 and 60% lower than control cells, respectively (Fig. 9 A, left dataset). Removal of ATP from the extracellular solution for 5 min caused PIP and $PI(4,5)P_2$ to fall by ∼80%, and the fall was still more pronounced for $PI(4,5)P_2$ when AMP-PNP was included in the extracellular solution. Addition of 2 mM Ca to the extracellular solution for 2 min resulted in almost no change of PIP levels but complete depletion of $PI(4,5)P_2$ (Fig. 9 A, right dataset).

Fig. 9 B shows our measurements of acylglycerols (M/DAG) and phosphatidic acid, using diacylglycerol kinase to generate phosphatidate and lysophosphatidate from acylglycerols (Preiss et al., 1987). In preliminary experiments, we established that the bacterial DAG kinase employed in this assay converted both 1-*O*-palmitylglycerol and dipalmitylglycerol, in amounts >3-fold greater than determined for cell lysates to phosphorylated metabolites that were recovered quantitatively as glycerol phosphate in our HPLC assay of anionic phospholipid metabolites. As shown in Fig. 9 B, the total di- and monocylglycerol content of BHK cells is similar to that of phosphatidate, namely 6–8% of total anionic phospholipid. For orientation, this is six to eight times more than the content of $PI(4,5)P_2$. As described in the left four bars, the addition of Ca to generate a free concentration of 0.4 mM in the extracellular medium, containing 2 mM MgATP, caused a 30% decrease of acylglycerol and a 15% increase of phosphatidate. These changes are consistent with diacylglycerol kinases being activated by Ca in these cells. Using cells with M1 receptors, we did not obtain significant effects of carbachol (0.3 mM) on acylglycerol levels, while phosphatidate increased by 15%. In response to the combined application of 0.4 mM free Ca and carbachol (0.3 mM), acylglycerol levels increased by 40% and phosphatidate levels increased by 24%. Finally, as shown in the right four bars of Fig. 9 B, incubation of cells with AMP-PNP (2 mM) instead of ATP caused a decrease of acylglycerol. In the presence of AMP-PNP, application of Ca (0.4 mM) for 1 min caused an increase of acylglycerol by 12% with no change of phosphatidate. While the increase is small, as a relative change, the absolute change is in fact larger than the entire $PI(4,5)P_2$ mass of the cells, and we point out that the increase of acylglycerol was accompanied by a significant decrease of phosphatidylinositol (unpublished data). Since PIP and $PI(4,5)P_2$ are depleted and cannot be synthesized in this condition, phospholipases evidently cleave significant amounts of phosphatidylinositol. In summary, these biochemical data demonstrate first that high cytoplasmic Ca indeed promotes generation of phosphatidic acid by activating DAG kinases, although this activity cannot explain the translocation of C1 domains into the cytoplasm described in Figs. 6 and 7. Second, they demonstrate that Ca might indeed support the generation of DAG on internal membranes from sources other than $PI(4,5)P_2$ in the circumstances of Figs. 6 and 7.

Further Evidence against Roles for PLC, PLD, and cPLA2 Activities, as well as other Ca-dependent Processes, in Membrane Fusion

Using the BHK cell line with high NCX1 expression, we tested a wide range of agents expected to change phosphatidylinositide metabolism, bind phosphatidylinositides, and/or inhibit phospholipases. All negative results reported here without figures reflect at least three and usually six or more control and treatment observations. We found no significant inhibition of membrane fusion or the rate of fusion by any of the following agents when included in the pipette solution and when fusion was quantified as a percent change of capacitance and related to the peak exchange current density: U73122 (10 μM), edelfosine (10 μM), nitrocoumarin (20 μM), neomycin (30 μM), heptalysine (40 μM), and 2000 MW polylysine (20 μM) to inhibit PLCs and/or bind $PI(4,5)P_2$ and other anionic phospholipids (Ben-Tal et al., 1996; Bucki et al., 2000), IP_3 (0.1 mM) to release PLC-δ from the membrane (Cifuentes et al., 1994), wortmannin (4 μM) to inhibit PI3- and type III PI4-kinases (Nakanishi et al., 1995), adenosine (1 mM) to inhibit type II PI4-kinases (Barylko et al., 2001), phosphatidylinositol transfer protein from yeast (0.1 mg/ml) to remove phosphatidylinositol from cell membranes (Routt and Bankaitis, 2004), recombinant

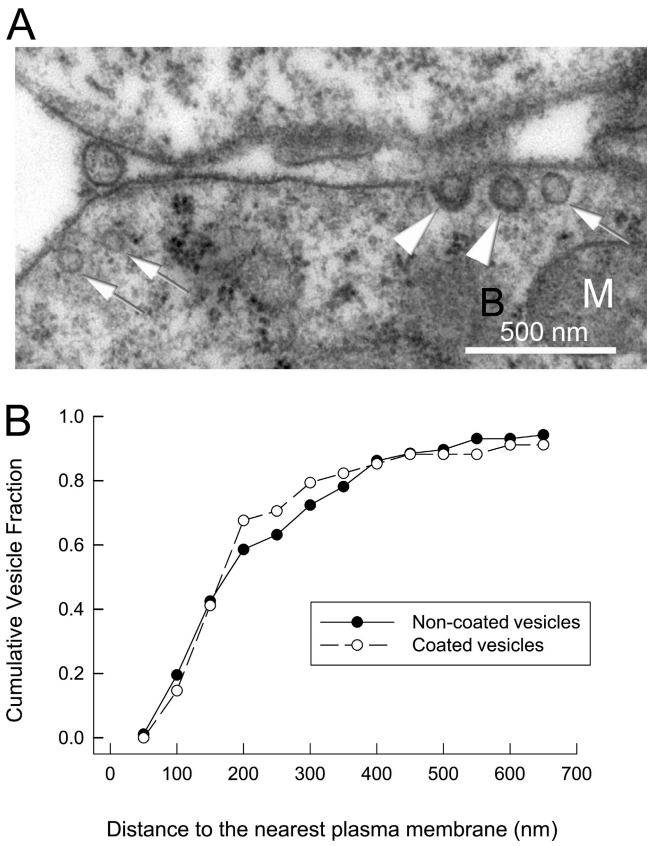

Figure 10. Electron microscopic analysis of BHK cell vesicles in close proximity to the surface membrane. (A) Electron micrograph of submembrane vesicles in a BHK cell. (B) Analysis of noncoated and coated vesicle numbers identified at the given distances from the surface membrane of >20 cells.

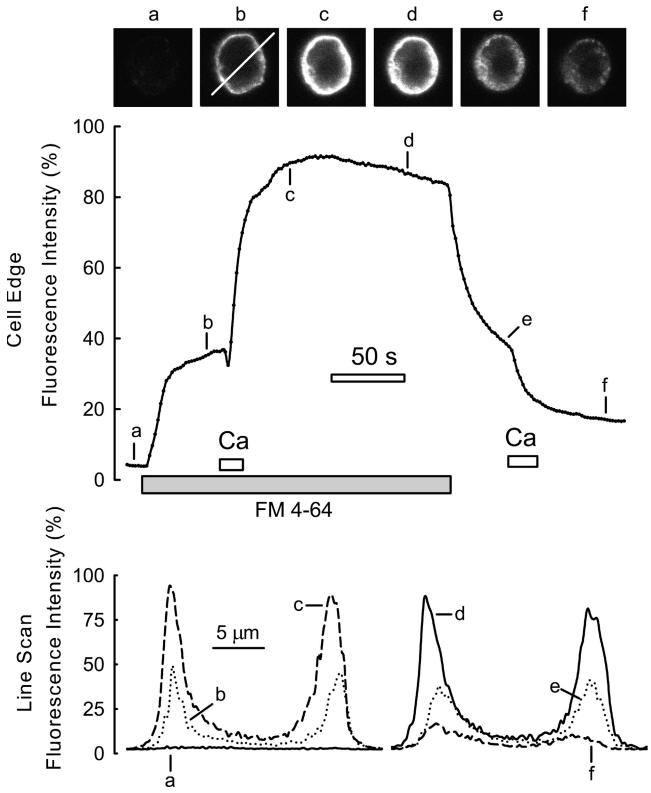

Figure 11. Typical staining and destaining in response to Ca influx in a BHK cell expressing NCX1. Background fluorescence without dye is negligible. After incubating the cell with 10 μM FM 4-64 for 50 s, Ca influx was activated for 10 s. Thereafter, fluorescence at the cell surface is greatly increased. Upon washing out the FM dye after 2.2 min, fluorescence declines by 60%. When Ca is introduced briefly a second time, fluroescence decreases rapidly by ~55%. This decrease corresponds to 28% of the total cell fluorescence before dye washout. Fluorescence micrographs and line scans at the time points indicated are provided above and below the fluorescence graph, respectively.

C1A domains (20 μM) to bind DAG (Colon-Gonzalez and Kazanietz, 2006), 0.6% butanol to stop DAG generation from phosphatidate (Choi et al., 2002), and a putatively specific phenylacrylamide cPLA2 inhibitor (Calbiochem #525143, 2 μM; Seno et al., 2000). The fact that exchange currents are not inhibited by agents that bind anionic phospholipids may appear surprising. The likely reason is that in these protocols there are no extracellular NCX1 ligands present until Ca is applied. Therefore, exchangers orient with ion transport sites open to the outside, and this configuration does not support the Na-dependent inactivation (Matsuoka and Hilgemann, 1994). We also tested for possible roles of other Ca-dependent processes. A possible role of Ca-activated microfilament depolymerization seems unlikely because phalloidin (5 μM) had no significant effect when perfused into cells for 5 min before activating Ca influx. A role of Ca-dependent proteolysis by calpain (Demarchi and Schneider, 2007) seems unlikely because high concentrations of a peptidic calpain inhibitor IV (20 μM, Calbiochem) had no significant effect when added to the cytoplasmic solution. A role of Ca-activated free radical generation seems unlikely because multiple free radical scavengers (TEMPO, 5 mM; sucrose, 40 mM; dithiothreitol, 2 mM; acetylcysteine, 2 mM; and ascorbate, 4 mM) were without significant effect in these protocols at concentrations suggested in the literature to suppress free radical signaling.

Failure to Correlate Capacitance Changes with Transporter or Channel Activity Changes

The source of the membrane that traffics in these experiments is not well defined. In this connection, we tested whether Na/Ca exchange activities or Na/K pump activities might increase with membrane fusion or decrease with the subsequent fall of capacitance. To do so, we activated the transport currents very briefly by application of extracellular Ca or K, respectively, to determine if maximal activity increases with membrane fusion and/or decreases during the period of membrane retrieval. We found no evidence that these transporter activities followed the changes of membrane area inferred from capacitance changes. In addition, we

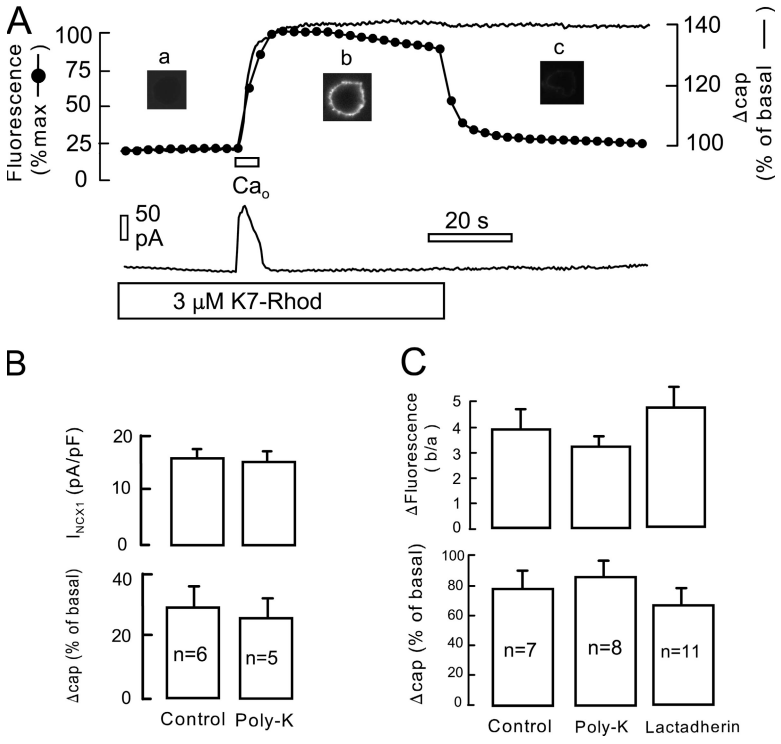

Figure 12. Extracellular cell surface accumulation of K7-Rhod (3 μM) upon activating maximal Ca influx in an NCX1-expressing BHK cell. (A) Cell membrane fluorescence and whole cell capacitance changes during and after application of 2 mM Ca for 5 s. Both the control and the Ca-containing solutions contain K7-Rhod. Fluorescence increases with nearly the same time course as membrane capacitance, and the K7-Rhod probe washes off the cell rapidly 45 s after activating Ca influx. Note that the background fluorescence of the light intensities given in the graph (∼20%) represents the homogeneous fluorescence of K7-Rhod throughout the solution. (B) Average peak exchange currents and membrane capacitance changes in response to 5 s application of Ca for six control cells and six cells perfused with 20 μM 2000 MW polylysine. Results are not significantly different. (C) Fluorescence and membrane capacitance changes, determined as in A, for 7 control cells, 8 cells perfused with 20 μM 2000 MW polylysine, and 11 cells perfused with 0.2 μM lactadherin.

performed similar experiments in cells expressing ROMK-type potassium channels (Zeng et al., 2003), and results were similarly negative.

Evidence for Membrane Fusion as the Cause of Ca-induced Capacitance Increase

The fact that phospholipase inhibitors had little or no effect on membrane fusion tends to eliminate the possibility that large biochemical changes could be causing dielectric changes in these experiments. Nevertheless, the large magnitudes of capacitance responses, in some cases doubling cell capacitance, do raise questions about the nature of the membrane fusing. Therefore, we performed an ultrastructural study to analyze subplasmalemmal vesicles and membrane structures in BHK cells that might participate in fusion events within 2–5 s of activating Ca influx. Cells were trypsinized and removed from plates, as in preparation for electrophysiological experiments. Cells were then fixed under conditions established previously for ultrastructural studies of submembrane compartments in neurons (see Materials and methods). As shown in Fig. 10, electron micrographs indeed show the presence of numerous vesicles within short distances of the surface membrane, both coated and uncoated vesicles with diameters ranging from 45 to 90 nm. In >20 cells examined, the distributions of noncoated and coated vesicles were found to be similar in dependence on distance from the membrane. Assuming that sections are 65 nm thick, we counted the numbers of vesicles per linear micron of membrane within 500 nm of the membrane, and we projected an average number of vesicles per square micron of membrane. With an average diameter of 80 nm, fusion of at least 50 vesicles per square micron would be required to double membrane area. Our estimate of vesicular densities was only ∼10% of this value, indicating an important discrepancy between ultrastructural analysis and functional results. Some possible explanations are that (1) vesicles are lost during the procedures employed, (2) vesicles fuse during the fixation protocols employed, and that (3) the vesicle population that fuses is generated during procedures to establish whole-cell voltage clamp. We mention that pipette perfusion of the fixative solutions into cells did not cause membrane fusion, based on capacitance recording.

It is beyond the scope of this article to determine the source of the discrepancy just outlined. Rather, we used optical methods to examine membrane cycling per se in these protocols with a hydrophobic fluorescence dye used in neuronal membrane cycling studies (e.g., Klingauf et al., 1998; Pyle et al., 1999). Fig. 11 shows typical results for the dye, FM 4–64 (Cochilla et al., 1999), which binds and dissociates rapidly from membranes and fluoresces only when bound. In preliminary studies, we labeled BHK cells with FM 4-64 for periods of minutes to several hours with the expectation that destaining might be observed during the activation of membrane fusion. However, in our experience compartments close to the surface membrane were not well labeled with FM dye, and there was little destaining upon activating Ca influx in voltage-clamped cells. From these results, we conclude that the membrane that cycles

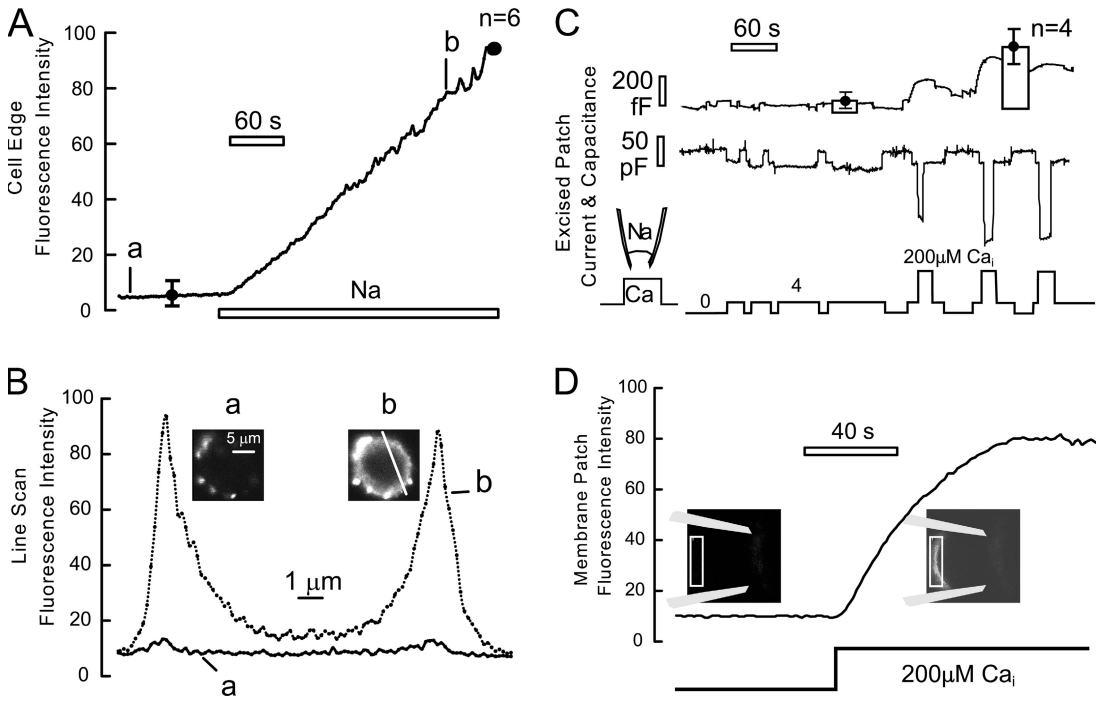

Figure 13. Extracellular cell surface accumulation of annexin-V Alexa Fluor 488 conjugate in response to increasing cytoplasmic Ca and activation of membrane fusion. In A and B, pipette perfusion of 40 mM Na was used to activate outward exchange current with 2 mM extracellular Ca and 1:100 annexin-V dilution. The pipette solution initially contains 40 mM Li. After recording background for 2 min, lithium is substituted for 40 mM Na via pipette perfusion through a 40-μm inner diameter quartz capillary. Panel A shows the surface membrane fluorescence, and B shows line scans of the cell before (solid line) and 5 min after activating exchange current. (C) Inward exchange current and capacitance responses induced in giant excised BHK patches by applying cytoplasmic solutions with 4 and 200 μM free Ca. The pipette contains 140 mM Na, and the pipette tip is switched between three solutions, as indicated. Capacitance responses are negligible on applying 4 μM free Ca. Two applications of 200 μM free Ca result in a total 300 fF increase of patch capacitance, estimated to be ∼10% of the initial patch membrane capacitance. (D) Extracellular binding of annexin-V Alexa Fluor 488 to the extracellular surface of a giant excised BHK patch upon applying 200 μM free Ca to the cytoplasmic surface. The pipette solution contains 2 mM extracellular Ca with 1:100 annexin-V dilution.

in voltage clamp experiments does not normally cycle in these cells, but rather is available as a membrane reserve in response to massive Ca influx, as expected with cell wounding.

Next, therefore, we performed experiments to label and destain BHK cells during voltage-clamp experiments, and Fig. 11 shows typical fluorescence records. Images and line scans used to determine the cell surface fluorescence are shown below the figure. Background fluorescence at the onset of the experiment was negligible, and FM 4-64 (10 μM) was applied and membrane fluorescence increased to a steady state with a time constant of a few seconds. After applying Ca to induce membrane fusion there was a large further increase of fluorescence with a time constant of about a minute. As described subsequently, this increase reflects, at least in part, internalization of membrane in parallel with presentation of new membrane for staining. However, after 2.2 min, the majority of the increase in fluorescence in response to Ca is rapidly reversed upon removing dye. Thus, a large part of the signal does not reflect membrane fusion and internalization, but rather a changed affinity of the dye to the extracellular membrane leaflette. Given that this dye is a divalent cation, the increased dye binding in response to membrane fusion may indicate that the extracellular membrane surface becomes anionic during membrane fusion. This explanation is supported by further experimentation described in Figs. 12 and 13. As apparent in Fig. 11, ∼30% of the total dye fluorescence typically did not wash out in these experiments after inducing membrane fusion and continuing dye application for 2 or more minutes. The remaining fluorescence after washout (e), which is roughly equivalent to the initial fluorescence on applying dye (b), is decreased by >50% upon applying a second pulse of Ca. This result suggests that the membrane that is internalized after the first Ca pulse can be fused again to the cell surface in response to a second pulse of Ca, as expected from the reversibility of capacitance changes in these experiments.

On the Nature of Cell Surface Changes during Membrane Fusion

The extracellular cell surface might become anionic for three reasons during protocols with massive Ca influx. First, high cytoplasmic Ca activates phospholipid

transport proteins (flipases) that cause phospholipid randomization between monolayers with externalization of PS (Bevers et al., 1999; Balasubramanian and Schroit, 2003). In this same connection, most models of membrane fusion require that, in order to achieve fusion of opposing membranes, transitional hemifused membrane structures must form in which nonbilayer structures exist (Siegel, 1999; Kozlovsky and Kozlov, 2002; Markin and Albanesi, 2002). Such structures may facilitate phospholipid translocation across monolayers (Homan and Pownall, 1988; Fattal et al., 1994). Second, it is possible that the lumen of vesicles that fuse contain large quantities of anionic phospholipids and/or anionic sugars that become part of the extracellular membrane monolayer during fusion. And third, membrane proteins in the vesicles that fuse might contain unusually high numbers of anionic residues that can bind and/or interact with FM dye. With this background, we tested whether another fluorescent polyvalent cation might bind to the extracellular surface of BHK cells during the Ca response, similar to the FM dye. Fig. 12 A shows cell-associated fluorescence changes with 3 μM rhodamine-labeled heptalysine (K7-Rhod) in the extracellular solutions. Fluorescence of the K7-Rhod solutions was significant, and fluorescence at the edges of voltage-clamped cells incubated with K7-Rhod was nearly indistinguishable from this background (see "a" in Fig. 12 A). Upon initiating Ca influx by application of 2 mM extracellular Ca, fluorescence rose in 5 s to a high level that is about five times greater than the solution background. The time course of the fluorescence rise nearly mimicked the time course of membrane fusion. As illustrated further in Fig. 12 A, fluorescence washed off nearly completely within 10 s, indicating that the increase of fluorescence is caused by increased binding at the extracellular cell surface.

To address the different possible mechanisms just outlined, we reasoned that the presence of agents that bind PS on the cytoplasmic side would decrease and/or slow the appearance of anionic groups on the outside if PS randomization were a significant factor. Therefore, we perfused cells with two agents that would be expected to bind PS significantly. To bind PS nonselectively, 2000 MW polylysine (20 μM) was added to the perfusion solution. As shown for an initial set of experiments in Fig. 12 B, the presence of cytoplasmic polylysine did not significantly decrease the peak exchange current or the percent increase of cell capacitance upon activating exchange current. As shown in Fig. 12 C for another set of experiments with optical recording, the increase of heptalysine binding on the extracellular side was unaffected by the presence of polylysine on the cytoplasmic side. Lactadherin (Shi et al., 2004) is a milk protein that binds PS with high affinity in a Ca-independent manner. To bind PS selectively, therefore, purified lactadherin was added to the cytoplasmic solution at a concentration of 0.2 μM, well above its K_d for PS (Shi et al., 2004), and cells were perfused with this solution for 3 min before activating exchange current. As shown in Fig. 12 C, the increase of heptalysine binding on the extracellular side was unaffected by the presence of lactadherin on the cytoplasmic side.

To address specifically whether PS increases in the outer monolayer of BHK cells, we monitored the binding of fluorescently labeled annexin-V (annexin-V Alexa Fluor 488; 530BP) to cells, bearing in mind two limitations. First, annexins require Ca to bind PS (Maffey et al., 2001) so that experiments must be performed entirely in the presence of extracellular Ca. Second, while several annexins bind PS selectively (Ravanat et al., 1992; Maffey et al., 2001; Kastl et al., 2002), the association rates appear to be rather low so that binding occurs with time constants on the order of 1 min (Blackwood and Ernst, 1990). Fig. 13 describes results from both whole-cell recording and from giant excised membrane patches. Fig. 13 (A and B) show the time course (A) and distribution of annexin binding to voltage-clamped BHK cells when outward exchange current is activated by perfusing Na (40 mM) into cells via pipette perfusion in substitution for Li (2 mM extracellular Ca with annexin-V Alexa Fluor 488 at 1:100 dilution). Annexin-V begins to bind to the outer cell surface abruptly and continues almost linearly for the duration of the recording. In six experiments, the cell surface fluorescence increased by >10-fold during Na perfusion. For the statistical analysis in Fig. 13 A, the cell membrane fluorescence after 2 min annexin-V incubation without Na was normalized to the fluorescence after perfusion of Na for 5 min. As evident in the micrographs in Fig. 13 B, staining was typically not uniform. Patches of annexin-V fluorescence are evident before inducing Ca influx. During the Ca influx period, staining becomes concentrated in areas that probably represent cell membrane blebs.

Although annexin binding takes many seconds in simple assays, it is striking that binding in these experiments shows no sign of saturation over more than 4 min after activating Ca influx. Thus, the extracellular appearance of PS might be slower than the binding of cationic agents, as described in the previous figures. To allow a more adequate kinetic analysis with well controlled Ca concentrations on the cytoplasmic side, we performed similar experiments using giant excised membrane patches. As described in an accompanying article (Wang and Hilgemann, 2008), large "releasable" pools of membrane vesicles can be maintained in excised giant patches. Fig. 13 C shows a typical recording from a BHK cell patch with statistics for four patches in which inward exchange currents and capacitance changes were monitored in response to rapidly applying cytoplasmic Ca. In brief, we find that it is possible to maintain a fusable membrane pool in BHK patches in which membrane

rises quite high in the pipette tip and by taking precautions to excise patches gently. As indicated below the records, inward exchange currents were first activated multiple times by 4 μM free Ca, whereby the patch capacitance remains stable. Thereafter, solution was switched three times from the one with 4 μM free Ca to one with 200 μM. This Ca concentration activates the maximal exchange current, and patch capacitance increases during the first two high Ca exposures.

As shown in Fig. 13 D, annexin-V binding from within the patch pipette tip indeed increases rather rapidly in this protocol. To monitor annexin-V binding, excised patches were positioned nearly horizontal to the stage to allow imaging of the pipette tip. Before applying Ca to the cytoplasmic membrane face, fluorescence of the annexin-V conjugate is negligible in the pipette tip. Upon cytoplasmic application of 200 μM free Ca, membrane in the patch pipette becomes well defined by annexin fluorescence with a time constant of ∼50 s (three similar observations), substantially faster than in whole cell experiments. Thus, we conclude that PS appearance in the extracellular cell surface may indeed occur rapidly with membrane fusion, and that the experiments with pipette perfusion of Na (Fig. 13 A) are compromised by the use of pipette perfusion to activate Ca influx.

DISCUSSION

We have characterized a Ca-activated membrane fusion mechanism in BHK fibroblasts that can increase membrane surface area by 25–100% in just a few seconds. In parallel, PLCs cleave the bulk of cellular $PI(4,5)P_2$ and possibly substantial amounts of PI, and the extracellular cell surface evidently becomes markedly anionic. The molecular mechanisms and relationships of these responses, which are discussed here, are of substantial interest from multiple biological and biophysical perspectives.

Massive Membrane Fusion via Low Affinity Ca Sensing in BHK Cells

This study extends previous work in which "caged Ca" was used to induce large Ca transients in CHO cells (Coorssen et al., 1996). Clearly, the magnitudes of Ca-induced capacitance changes in fibroblasts can match or exceed those occurring in cells with profuse neurotransmitter release (Kilic, 2002; Bauer et al., 2007; Zeniou-Meyer et al., 2007). In this study, the responses begin with a longer delay (100–500 ms) than described for flash photolysis, as expected to allow cytosolic Ca accumulation by Ca transport. Differently from the flash photolysis studies, we routinely observe an initial decrease of capacitance during which the conductance signal component increases. One possible explanation is that the negative capacitance phase reflects hemifusion of a large population of vesicles, as predicted from most membrane fusion models (Siegel, 1999; Kozlovsky and Kozlov, 2002; Markin and Albanesi, 2002), whereby transmembrane voltage might transiently become divided across two membranes in series. For reasons outlined with the Results, transient conductance components in our records (Fig. 1) are likely to reflect the generation of "fusion pores" during the fusion process (Lindau and Alverez de Toledo, 2003), although we cannot entirely eliminate some contribution from changes of transporter function that do not mirror the exchange current per se.

Using a low affinity Ca indicator, we find that free cytoplasmic Ca peaks at ∼0.2 mM with peak outward exchange currents of 0.1–0.2 nA activated for 2–4 s in cells of 15–30 pF (Fig. 2). Since the rate of rise of capacitance increases over the entire range of exchange currents that can be activated (Fig. 3), it seems certain that the affinity of the underlying Ca sensor is rather low. In experiments in which the maximal free cytoplasmic Ca was thermodynamically capped by using equal cytoplasmic and extracellular Na concentrations (Fig. 3, C and D), the half-maximal free Ca to activate the fusion response is estimated to be 140 μM, and this approximate K_d is consistent with results from excised patches described in Fig. 13 C and in an accompanying article (Wang and Hilgemann, 2008). As demonstrated in Fig. 3 B, clear increases of cell capacitance can nevertheless be detected when free cytoplasmic Ca is limited to not exceed 10 μM (i.e., with 40 mM Na on both membrane sides). This is readily explained if the Ca dependence of the fusion process has only weak cooperativity, as determined here and in the accompanying article (Wang and Hilgemann, 2008), in comparison to that observed for neurotransmitter release in neurons (Schneggenburger and Neher, 2005). In fact, the Hill coefficients given in Fig. 3 (2.2 and 2.1) may be an overestimate because Ca buffering by EGTA (0.5 mM) can dampen the rise of free Ca when exchange currents are small. Given the low Ca cooperativity, it is plausible that the fusion mechanism analyzed here can be weakly activated by physiological Ca transients, in addition to Ca influx via cell wounds. Both the apparent Ca affinity ($K_d \sim 120$ μM) and the low cooperativity of responses (Hill coefficients of ∼2) are similar to those determined for asynchronous neurotransmitter release in neurons (Sun et al., 2007). Finally, it seems notable that the maximal fusion rate (i.e., $dCap/dt$) decreases from one Ca influx episode to the next, while the maximal capacitance increase does not decrease. Our explanation is that the rundown of fusion simply reflects the rundown of exchange currents used to activate the response. Thus, the fusion mechanism itself seems to be highly resistant to washout of soluble cell proteins, although it is modestly suppressed over several minutes by substitution of ATP for a nonhydrolyzable ATP analogue (Fig. 5).

Several additional observations seem fundamental. First, the capacitance responses can reverse completely and can be repeated several times in the same cell (Fig. 1). In the context of this article, it must suffice to summarize that the reversal is somewhat variable. Reversal was often only partial (e.g., Fig. 4), but it could also exceed the initial membrane fusion response when allowed to progress unabated after a short episode of Ca influx. Second, we analyzed functionally whether any conductances readily analyzed, including Na/K pumps, Na/Ca exchange, and some K channels, traffic with the membrane that cycles during these responses, and our outcomes were negative in all of these cases. A long-term increase of cell conductance that often occurs with each fusion episode (e.g., Fig. 1) probably reflects a decrease of the seal resistance. It would seem that membrane proteins that enter the surface membrane during fusion can be subsequently internalized without mixing with the bulk of membrane proteins in the cell surface, even during multiple fusion-retrieval episodes. This indirect conclusion is similar to conclusions for membrane cycling during neurotransmitter release (Willig et al., 2006) that are presently under debate (Wienisch and Klingauf, 2006), and we stress that this conclusion may not apply at all to membrane phospholipids. Third, it is revealing that the membrane compartment that cycles could not be labeled by preincubating cells with FM dyes. This observation suggests that the membrane compartment(s) that fuse to the surface do not traffic under standard cell culture conditions. Fourth, we have demonstrated that substantial numbers of vesicles are in close proximity to the surface membrane of rounded BHK cells, removed from dishes (Fig. 10), but the quantities of vesicles are not adequate to account for the fusion responses. Further work with different approaches will clearly be essential to account for the membrane that cycles in response to Ca influx. Fifth, although we did not provide detailed analysis, it is our routine observation that the second fusion response is larger and/or faster than the first response (e.g., Fig. 1). This "facilitation" of fusion may reflect the same facilitation observed for wound healing per se in other cell types, whereby the rate of healing is approximately doubled at a second response (Togo et al., 2003; Steinhardt, 2005).

Ca-dependent PLC Activation in BHK Cells Appears to be Unrelated to the Initiation of Membrane Fusion

As outlined in the Introduction, both DAG and $PI(4,5)P_2$ may modulate membrane fusion events by multiple mechanisms. As noted in connection with Fig. 6, the cytoplasmic Ca concentrations needed to activate fusion at half-maximal rates are probably greater than those needed to activate PLCs in BHK cells without receptor activation. As noted further with those Results, we could clearly detect PLC activities with 10 μM free cytoplasmic Ca, a concentration that causes membrane fusion at only very low rates (Fig. 3). Overall, our work appears to negate any role of PLCs in this type of membrane fusion when Ca influx is massive. The fusion responses were unaffected by depletion of $PI(4,5)P_2$ (e.g., by receptor activation in Fig. 7) and the parallel generation of DAG. Activation of M1 receptors by carbachol can initiate small increases of capacitance (Fig. 7 C), and as described previously (Yaradanakul et al., 2007), but subsequent Ca influx still activates massive membrane fusion (Fig. 7). And finally, responses to maximal Ca influx were unaffected by multiple agents known to inhibit PLCs (U73122, edelfosine, neomycin, or heptalysine), as well as by pipette perfusion of DAG-binding C1 domains, agents that circumvent DAG generation via PLD pathways, namely 0.6% butanol (Choi et al., 2002), and agents that are expected to bind $PI(4,5)P_2$ as well as other anionic phospholipids (Fig. 12). At this time, we cannot entirely discount roles for phosphoinositides and/or DAG-dependent mechanisms in long-term regulation of this type of fusion, or a role in setting the Ca dependence of fusion. Clearly, ATP-dependent processes do affect the maximal fusion amplitude (Fig. 5), and these are addressed further in an accompanying article (Wang and Hilgemann, 2008).

Our imaging results for PH and C1 fusion proteins allow comparisons of responses to receptor activation and Ca elevation (Figs. 6 and 7). PH domains respond to a large increase of cytoplasmic Ca just as rapidly as they respond to receptor activation, and in experiments at 35°C the domains reequilibrate after brief PLC activation with a time constant of ~1 min. These time courses are likely to reflect the turnover rate of $PI(4,5)P_2$ in these cells. As pointed out in Results, the C1 domains reequilibrate somewhat more slowly after brief activation of PLCs. Of most interest, Ca influx clearly has dual influences on the distribution of C1 domains. When C1 domains are brought to the surface membrane by multiple means (Figs. 6 and 7), Ca influx causes rapid translocation of the C1 domains back to the cytoplasm with a time constant of <1 min, and multiple results argue against metabolism of DAG being the cause of C1 translocation. DAG kinase inhibitors were without effect, results were similar with PMA (Fig. 7), which cannot be metabolized, and results were similar when cells were perfused with nonhydrolyzable ATP analogues.

Anionic Phospholipids and Membrane Fusion

The present results are relevant to several open questions about anionic phospholipids in membrane fusion. Since the cytoplasmic Ca requirements for membrane fusion in BHK cells are quite high, the binding of Ca by anionic phospholipids can be considered as a possible trigger for fusion. In fact, the fusion of anionic vesicles composed of purified phospholipids can show a significant degree of selectivity for Ca versus Mg in the concentration range occurring in the present experiments

(Newton et al., 1978; Duzgunes et al., 1981; Summers et al., 1996), and furthermore, Ca binding to PS-containing bilayers brought into close apposition can occur with both high selectivity and affinity (Feigenson, 1986; Feigenson, 1989). Our results contradict this possibility because membrane fusion is unaffected by agents that bind PS (polylysine and lactadherin in Fig. 12), as well as other anionic phospholipids, and would be expected to sequester them away from other binding partners. It would be interesting to know if C1 domains, which bind PS as well as DAG (Johnson et al., 2000; Bittova et al., 2001), might be released from cell membranes by these PS binding agents. As evident in Fig. 7 (B and C), the shift of C1 domains to the cytoplasm in response to Ca influx can reverse very rapidly when Ca influx is terminated, as expected if fast Ca dissociation from anionic phospholipids favors C1 binding to the membrane.

At present we have not entirely eliminated one alternative explanation for the Ca-dependent movement of C1 domains. As shown by mass measurements of phospholipids, mono- and/or diacylglycerols increase with high cytoplasmic Ca, even after $PI(4,5)P_2$ depletion by receptor activation or removal of ATP (Fig. 9 B). If DAG increases markedly when Ca rises, DAG on internal membranes might draw C1 domains away from the surface membrane. One argument against this idea is that total basal DAG levels appear to be higher than $PI(4,5)P_2$ levels, as in other cell types (Callender et al., 2007), and therefore DAG concentrations in internal membranes may already be high in the basal state. A second argument against this idea is that the C1 domains appear uniformly distributed in the cytoplasm after activating Ca influx, as expected if they are not associated with specific membrane compartments.

From the extracellular side, it is striking that the affinity of cationic agents for the extracellular cell surface increases profoundly and rapidly with membrane fusion (Figs. 11 and 12). As pointed out in Results, there are multiple possible explanations. If PS is translocating from the cytoplasmic leaflet to the extracellular membrane leaflet, for example as a result of nonbilayer structures occurring during membrane fusion, one would expect that agents that bind PS would slow and/or inhibit the process when applied from the cytoplasmic side. As shown in Fig. 12 that was not the case for either polylysine or the PS-binding protein lactadherin. Annexin-V binds much more slowly to the extracellular surface than the cationic agents in whole cell recording (Fig. 13, A and B), suggesting that PS may appear more slowly than membrane fusion occurs. However, the annexin results are not definitive. First, whole-cell experiments are limited by the fact that Ca must be present on the outside to allow annexin binding. Using cell perfusion of Na to activate Ca influx, it is certain that Ca transients are slower and of lower magnitude than for rapid activation of reverse exchange currents. Second, kinetic studies of annexin binding to PS-containing membranes indeed show rather slow kinetics (Blackwood and Ernst, 1990; Kastl et al., 2002). Thus, the results may be kinetically limited by the rate of annexin-V binding. In fact, annexin-V binds substantially faster to the extracellular surface of giant excised patches, when Ca is rapidly applied to the cytoplasmic side (Fig. 13 D), than occurs in the whole cell experiments. Together, the results of Figs. 12 and 13 would suggest that PS does not translocate from the cytoplasmic leaflet but rather may appear in the extracellular surface immediately as a result of membrane fusion, as expected if the inner leaflet of the membranes of vesicles that fuse is anionic. Clearly, this suggestion requires more experimentation in which means are found to inhibit membrane fusion selectively without inhibiting Ca transients. We point out that extracellular PS exposure has been described previously in mast cells in response to degranulation (Demo et al., 1999; Martin et al., 2000) and in auditory hair cells in association with membrane cycling (Shi et al., 2007). Similar to the present study, it is an open question in both of those studies whether PS "translocates" from the cytoplasmic leaflet of the surface membrane during fusion or whether it enters the extracellular cell surface monolayer from the luminal monolayer of vesicles. A parallel problem in red blood cells is that phospholipid scrambling can be associated with membrane shedding. To account for membrane shedding, a membrane "division" process must occur in which transiently nonbilayer membrane structures are generated (Comfurius et al., 1990).

In summary, we have analyzed in more detail than heretofore massive membrane fusion at the cell surface of a standard immortalized fibroblast in response to a rapid increase of cytoplasmic Ca. The activation of PLCs that occurs in parallel appears to be unrelated to the fusion process and does not modulate it to any significant degree in our experiments with massive Ca influx. Our results to date are consistent with membrane fusion causing the appearance of anionic phospholipids at the extracellular surface by a mechanism that does not involve PS "scrambling" between monolayers. Our results provide no support for any specific or nonspecific role of "signaling" phospholipids in this type of membrane fusion or its triggering by Ca.

We thank Marc Llaguno (University of Texas Southwestern Medical Center at Dallas) for critical discussions and advice, Kenneth D. Philipson (University of California, Los Angeles, CA) for the BHK cell line, NCX1 reagents and discussions, Mark Shapiro (University of Texas at San Antonio, TX) for hM1 constructs employed, and Gary Gilbert (Harvard Medical School, Boston, MA) for lactadherin protein.

This work was supported by HL0679420 and HL051323 to D. W. Hilgemann.

Lawrence G. Palmer served as editor.

Submitted: 6 August 2007
Accepted: 25 April 2008

REFERENCES

Andrews, N.W. 2005. Membrane resealing: synaptotagmin VII keeps running the show. *Sci. STKE.* 2005:e19.

Andrews, N.W., and S. Chakrabarti. 2005. There's more to life than neurotransmission: the regulation of exocytosis by synaptotagmin VII. *Trends Cell Biol.* 15:626–631.

Bai, J., W.C. Tucker, and E.R. Chapman. 2004. PI(4,5)P2 increases the speed of response of synaptotagmin and steers its membrane-penetration activity toward the plasma membrane. *Nat. Struct. Mol. Biol.* 11:36–44.

Balasubramanian, K., and A.J. Schroit. 2003. Aminophospholipid asymmetry: a matter of life and death. *Annu. Rev. Physiol.* 65:701–734.

Bankaitis, V.A., and A.J. Morris. 2003. Lipids and the exocytotic machinery of eukaryotic cells. *Curr. Opin. Cell Biol.* 15:389–395.

Bansal, D., and K.P. Campbell. 2004. Dysferlin and the plasma membrane repair in muscular dystrophy. *Trends Cell Biol.* 14:206–213.

Barylko, B., S.H. Gerber, D.D. Binns, N. Grichine, M. Khvotchev, T.C. Sudhof, and J.P. Albanesi. 2001. A novel family of phosphatidylinositol 4-kinases conserved from yeast to humans. *J. Biol. Chem.* 276:7705–7708.

Bauer, C.S., R.J. Woolley, A.G. Teschemacher, and E.P. Seward. 2007. Potentiation of exocytosis by phospholipase C-coupled G-protein-coupled receptors requires the priming protein Munc13-1. *J. Neurosci.* 27:212–219.

Bement, W.M., C.A. Mandato, and M.N. Kirsch. 1999. Wound-induced assembly and closure of an actomyosin purse string in *Xenopus* oocytes. *Curr. Biol.* 9:579–587.

Ben-Tal, N., B. Honig, R.M. Peitzsch, G. Denisov, and S. McLaughlin. 1996. Binding of small basic peptides to membranes containing acidic lipids: theoretical models and experimental results. *Biophys. J.* 71:561–575.

Bevers, E.M., P. Comfurius, D.W. Dekkers, and R.F. Zwaal. 1999. Lipid translocation across the plasma membrane of mammalian cells. *Biochim. Biophys. Acta.* 1439:317–330.

Bittova, L., R.V. Stahelin, and W. Cho. 2001. Roles of ionic residues of the C1 domain in protein kinase C-α activation and the origin of phosphatidylserine specificity. *J. Biol. Chem.* 276:4218–4226.

Blackwood, R.A., and J.D. Ernst. 1990. Characterization of Ca^{2+}-dependent phospholipid binding, vesicle aggregation and membrane fusion by annexins. *Biochem. J.* 266:195–200.

Breitbart, H., and B. Spungin. 1997. The biochemistry of the acrosome reaction. *Mol. Hum. Reprod.* 3:195–202.

Brown, W.J., K. Chambers, and A. Doody. 2003. Phospholipase A2 (PLA2) enzymes in membrane trafficking: mediators of membrane shape and function. *Traffic.* 4:214–221.

Bucki, R., F. Giraud, and J.C. Sulpice. 2000. Phosphatidylinositol 4,5-bisphosphate domain inducers promote phospholipid transverse redistribution in biological membranes. *Biochemistry.* 39:5838–5844.

Callender, H.L., J.S. Forrester, P. Ivanova, A. Preininger, S. Milne, and H.A. Brown. 2007. Quantification of diacylglycerol species from cellular extracts by electrospray ionization mass spectrometry using a linear regression algorithm. *Anal. Chem.* 79:263–272.

Choi, S.Y., P. Huang, G.M. Jenkins, D.C. Chan, J. Schiller, and M.A. Frohman. 2006. A common lipid links Mfn-mediated mitochondrial fusion and SNARE-regulated exocytosis. *Nat. Cell Biol.* 8:1255–1262.

Choi, W.S., Y.M. Kim, C. Combs, M.A. Frohman, and M.A. Beaven. 2002. Phospholipases D1 and D2 regulate different phases of exocytosis in mast cells. *J. Immunol.* 168:5682–5689.

Cifuentes, M.E., T. Delaney, and M.J. Rebecchi. 1994. D-myo-inositol 1,4,5-trisphosphate inhibits binding of phospholipase C-δ1 to bilayer membranes. *J. Biol. Chem.* 269:1945–1948.

Cochilla, A.J., J.K. Angleson, and W.J. Betz. 1999. Monitoring secretory membrane with FM1-43 fluorescence. *Annu. Rev. Neurosci.* 22:1–10.

Colon-Gonzalez, F., and M.G. Kazanietz. 2006. C1 domains exposed: from diacylglycerol binding to protein-protein interactions. *Biochim. Biophys. Acta.* 1761:827–837.

Comfurius, P., J.M. Senden, R.H. Tilly, A.J. Schroit, E.M. Bevers, and R.F. Zwaal. 1990. Loss of membrane phospholipid asymmetry in platelets and red cells may be associated with calcium-induced shedding of plasma membrane and inhibition of aminophospholipid translocase. *Biochim. Biophys. Acta.* 1026:153–160.

Coorssen, J.R., H. Schmitt, and W. Almers. 1996. Ca^{2+} triggers massive exocytosis in Chinese hamster ovary cells. *EMBO J.* 15:3787–3791.

Czibener, C., N.M. Sherer, S.M. Becker, M. Pypaert, E. Hui, E.R. Chapman, W. Mothes, and N.W. Andrews. 2006. Ca^{2+} and synaptotagmin VII-dependent delivery of lysosomal membrane to nascent phagosomes. *J. Cell Biol.* 174:997–1007.

Demarchi, F., and C. Schneider. 2007. The calpain system as a modulator of stress/damage response. *Cell Cycle.* 6:136–138.

Demo, S.D., E. Masuda, A.B. Rossi, B.T. Throndset, A.L. Gerard, E.H. Chan, R.J. Armstrong, B.P. Fox, J.B. Lorens, D.G. Payan, et al. 1999. Quantitative measurement of mast cell degranulation using a novel flow cytometric annexin-V binding assay. *Cytometry.* 36:340–348.

Detrait, E.R., S. Yoo, C.S. Eddleman, M. Fukuda, G.D. Bittner, and H.M. Fishman. 2000. Plasmalemmal repair of severed neurites of PC12 cells requires Ca^{2+} and synaptotagmin. *J. Neurosci. Res.* 62:566–573.

DiPolo, R., G. Berberian, and L. Beauge. 2000. In squid nerves intracellular Mg^{2+} promotes deactivation of the ATP-upregulated Na^{+}/Ca^{2+} exchanger. *Am. J. Physiol. Cell Physiol.* 279:C1631–C1639.

Duzgunes, N., J. Wilschut, R. Fraley, and D. Papahadjopoulos. 1981. Studies on the mechanism of membrane fusion. Role of headgroup composition in calcium- and magnesium-induced fusion of mixed phospholipid vesicles. *Biochim. Biophys. Acta.* 642:182–195.

Fan, J.S., and P. Palade. 1998. Perforated patch recording with β-escin. *Pflugers Arch.* 436:1021–1023.

Fattal, E., S. Nir, R.A. Parente, and F.C. Szoka Jr. 1994. Pore-forming peptides induce rapid phospholipid flip-flop in membranes. *Biochemistry.* 33:6721–6731.

Feigenson, G.W. 1986. On the nature of calcium ion binding between phosphatidylserine lamellae. *Biochemistry.* 25:5819–5825.

Feigenson, G.W. 1989. Calcium ion binding between lipid bilayers: the four-component system of phosphatidylserine, phosphatidylcholine, calcium chloride, and water. *Biochemistry.* 28:1270–1278.

Fraley, R., J. Wilschut, N. Duzgunes, C. Smith, and D. Papahadjopoulos. 1980. Studies on the mechanism of membrane fusion: role of phosphate in promoting calcium ion induced fusion of phospholipid vesicles. *Biochemistry.* 19:6021–6029.

Geppert, M., Y. Goda, R.E. Hammer, C. Li, T.W. Rosahl, C.F. Stevens, and T.C. Sudhof. 1994. Synaptotagmin I: a major Ca^{2+} sensor for transmitter release at a central synapse. *Cell.* 79:717–727.

Goni, F.M., and A. Alonso. 2000. Membrane fusion induced by phospholipase C and sphingomyelinases. *Biosci. Rep.* 20:443–463.

Grishanin, R.N., J.A. Kowalchyk, V.A. Klenchin, K. Ann, C.A. Earles, E.R. Chapman, R.R. Gerona, and T.F. Martin. 2004. CAPS acts at a prefusion step in dense-core vesicle exocytosis as a PIP2 binding protein. *Neuron.* 43:551–562.

Gundersen, C.B., S.A. Kohan, Q. Chen, J. Iagnemma, and J.A. Umbach. 2002. Activation of protein kinase Cη triggers cortical granule exocytosis in *Xenopus* oocytes. *J. Cell Sci.* 115:1313–1320.

Harrison, R.A., and E.R. Roldan. 1990. Phosphoinositides and their products in the mammalian sperm acrosome reaction. *J. Reprod. Fertil. Suppl.* 42:51–67.

Haslam, R.J., and J.R. Coorssen. 1993. Evidence that activation of phospholipase D can mediate secretion from permeabilized platelets. *Adv. Exp. Med. Biol.* 344:149–164.

Ho, C., S.J. Slater, B. Stagliano, and C.D. Stubbs. 2001. The C1 domain of protein kinase C as a lipid bilayer surface sensing module. *Biochemistry.* 40:10334–10341.

Homan, R., and H.J. Pownall. 1988. Transbilayer diffusion of phospholipids: dependence on headgroup structure and acyl chain length. *Biochim. Biophys. Acta.* 938:155–166.

Howell, G.J., Z.G. Holloway, C. Cobbold, A.P. Monaco, and S. Ponnambalam. 2006. Cell biology of membrane trafficking in human disease. *Int. Rev. Cytol.* 252:1–69.

Jaiswal, J.K., S. Chakrabarti, N.W. Andrews, and S.M. Simon. 2004. Synaptotagmin VII restricts fusion pore expansion during lysosomal exocytosis. *PLoS Biol.* 2:E233.

Jiang, Y., W. Qian, J.W. Hawes, and J.P. Walsh. 2000a. A domain with homology to neuronal calcium sensors is required for calcium-dependent activation of diacylglycerol kinase α. *J. Biol. Chem.* 275:34092–34099.

Jiang, Y., F. Sakane, H. Kanoh, and J.P. Walsh. 2000b. Selectivity of the diacylglycerol kinase inhibitor 3-[2-(4-[bis-(4-fluorophenyl)methylene]-1-piperidinyl)ethyl]-2, 3-dihydro-2-thioxo-4(1H)quinazolinone (R59949) among diacylglycerol kinase subtypes. *Biochem. Pharmacol.* 59:763–772.

Johnson, J.E., J. Giorgione, and A.C. Newton. 2000. The C1 and C2 domains of protein kinase C are independent membrane targeting modules, with specificity for phosphatidylserine conferred by the C1 domain. *Biochemistry.* 39:11360–11369.

Jun, Y., R.A. Fratti, and W. Wickner. 2004. Diacylglycerol and its formation by phospholipase C regulate Rab- and SNARE-dependent yeast vacuole fusion. *J. Biol. Chem.* 279:53186–53195.

Kastl, K., M. Ross, V. Gerke, and C. Steinem. 2002. Kinetics and thermodynamics of annexin A1 binding to solid-supported membranes: a QCM study. *Biochemistry.* 41:10087–10094.

Katz, B. 2003. Neural transmitter release: from quantal secretion to exocytosis and beyond. *J. Neurocytol.* 32:437–446.

Kilic, G. 2002. Exocytosis in bovine chromaffin cells: studies with patch-clamp capacitance and FM1-43 fluorescence. *Biophys. J.* 83:849–857.

Klingauf, J., E.T. Kavalali, and R.W. Tsien. 1998. Kinetics and regulation of fast endocytosis at hippocampal synapses. *Nature.* 394:581–585.

Koumandou, V.L., J.B. Dacks, R.M. Coulson, and M.C. Field. 2007. Control systems for membrane fusion in the ancestral eukaryote; evolution of tethering complexes and SM proteins. *BMC Evol. Biol.* 7:29.

Kozlovsky, Y., and M.M. Kozlov. 2002. Stalk model of membrane fusion: solution of energy crisis. *Biophys. J.* 82:882–895.

Krause, T.L., H.M. Fishman, M.L. Ballinger, and G.D. Bittner. 1994. Extent and mechanism of sealing in transected giant axons of squid and earthworms. *J. Neurosci.* 14:6638–6651.

Latham, C.F., and F.A. Meunier. 2006. Munc18a: Munc-y business in mediating exocytosis. *Int. J. Biochem. Cell Biol.* 39:1576–1581.

Li, Y., N. Gamper, D.W. Hilgemann, and M.S. Shapiro. 2005. Regulation of Kv7 (KCNQ) K^+ channel open probability by phosphatidylinositol 4,5-bisphosphate. *J. Neurosci.* 25:9825–9835.

Linck, B., Z. Qiu, Z. He, Q. Tong, D.W. Hilgemann, and K.D. Philipson. 1998. Functional comparison of the three isoforms of the Na^+/Ca^{2+} exchanger (NCX1, NCX2, NCX3). *Am. J. Physiol.* 274:C415–C423.

Lindau, M., and G. Alverez de Toledo. 2003. The fusion pore. *Biochim. Biophys. Acta.* 1641:167–173.

Luo, B., D.S. Regier, S.M. Prescott, and M.K. Topham. 2004. Diacylglycerol kinases. *Cell. Signal.* 16:983–989.

Madison, J.M., S. Nurrish, and J.M. Kaplan. 2005. UNC-13 interaction with syntaxin is required for synaptic transmission. *Curr. Biol.* 15:2236–2242.

Maffey, K.G., L.B. Keil, and V.A. DeBari. 2001. The influence of lipid composition and divalent cations on annexin V binding to phospholipid mixtures. *Ann. Clin. Lab. Sci.* 31:85–90.

Markin, V.S., and J.P. Albanesi. 2002. Membrane fusion: stalk model revisited. *Biophys. J.* 82:693–712.

Martin, S., I. Pombo, P. Poncet, B. David, M. Arock, and U. Blank. 2000. Immunologic stimulation of mast cells leads to the reversible exposure of phosphatidylserine in the absence of apoptosis. *Int. Arch. Allergy Immunol.* 123:249–258.

Matsuoka, S., and D.W. Hilgemann. 1992. Steady-state and dynamic properties of cardiac sodium-calcium exchange. Ion and voltage dependencies of the transport cycle. *J. Gen. Physiol.* 100:963–1001.

Matsuoka, S., and D.W. Hilgemann. 1994. Inactivation of outward Na^+-Ca^{2+} exchange current in guinea-pig ventricular myocytes. *J. Physiol.* 476:443–458.

Maximov, A., and T.C. Sudhof. 2005. Autonomous function of synaptotagmin 1 in triggering synchronous release independent of asynchronous release. *Neuron.* 48:547–554.

Mayer, A. 2002. Membrane fusion in eukaryotic cells. *Annu. Rev. Cell Dev. Biol.* 18:289–314.

Mayer, A., D. Scheglmann, S. Dove, A. Glatz, W. Wickner, and A. Haas. 2000. Phosphatidylinositol 4,5-bisphosphate regulates two steps of homotypic vacuole fusion. *Mol. Biol. Cell.* 11:807–817.

Milosevic, I., J.B. Sorensen, T. Lang, M. Krauss, G. Nagy, V. Haucke, R. Jahn, and E. Neher. 2005. Plasmalemmal phosphatidylinositol-4,5-bisphosphate level regulates the releasable vesicle pool size in chromaffin cells. *J. Neurosci.* 25:2557–2565.

Nakanishi, S., K.J. Catt, and T. Balla. 1995. A wortmannin-sensitive phosphatidylinositol 4-kinase that regulates hormone-sensitive pools of inositolphospholipids. *Proc. Natl. Acad. Sci. USA.* 92:5317–5321.

Nasuhoglu, C., S. Feng, J. Mao, M. Yamamoto, H.L. Yin, S. Earnest, B. Barylko, J.P. Albanesi, and D.W. Hilgemann. 2002a. Nonradioactive analysis of phosphatidylinositides and other anionic phospholipids by anion-exchange high-performance liquid chromatography with suppressed conductivity detection. *Anal. Biochem.* 301:243–254.

Nasuhoglu, C., S. Feng, Y. Mao, I. Shammat, M. Yamamato, S. Earnest, M. Lemmon, and D.W. Hilgemann. 2002b. Modulation of cardiac PIP2 by cardioactive hormones and other physiologically relevant interventions. *Am. J. Physiol. Cell Physiol.* 283:C223–C234.

Neef, A., C. Heinemann, and T. Moser. 2007. Measurements of membrane patch capacitance using a software-based lock-in system. *Pflugers Arch.* 454:335–344.

Newton, C., W. Pangborn, S. Nir, and D. Papahadjopoulos. 1978. Specificity of Ca^{2+} and Mg^{2+} binding to phosphatidylserine vesicles and resultant phase changes of bilayer membrane structure. *Biochim. Biophys. Acta.* 506:281–287.

Oancea, E., M.N. Teruel, A.F. Quest, and T. Meyer. 1998. Green fluorescent protein (GFP)-tagged cysteine-rich domains from protein kinase C as fluorescent indicators for diacylglycerol signaling in living cells. *J. Cell Biol.* 140:485–498.

Papahadjopoulos, D., S. Nir, and N. Duzgunes. 1990. Molecular mechanisms of calcium-induced membrane fusion. *J. Bioenerg. Biomembr.* 22:157–179.

Preiss, J.E., C.R. Loomis, R.M. Bell, and J.E. Niedel. 1987. Quantitative measurement of sn-1,2-diacylglycerols. *Methods Enzymol.* 141:294–300.

Pyle, J.L., E.T. Kavalali, S. Choi, and R.W. Tsien. 1999. Visualization of synaptic activity in hippocampal slices with FM1-43 enabled by fluorescence quenching. *Neuron.* 24:803–808.

Rao, S.K., C. Huynh, V. Proux-Gillardeaux, T. Galli, and N.W. Andrews. 2004. Identification of SNAREs involved in synaptotagmin VII-regulated lysosomal exocytosis. *J. Biol. Chem.* 279:20471–20479.

Ravanat, C., J. Torbet, and J.M. Freyssinet. 1992. A neutron solution scattering study of the structure of annexin-V and its binding to lipid vesicles. *J. Mol. Biol.* 226:1271–1278.

Reddy, A., E.V. Caler, and N.W. Andrews. 2001. Plasma membrane repair is mediated by Ca^{2+}-regulated exocytosis of lysosomes. *Cell.* 106:157–169.

Rhee, S.G. 2001. Regulation of phosphoinositide-specific phospholipase C. *Annu. Rev. Biochem.* 70:281–312.

Routt, S.M., and V.A. Bankaitis. 2004. Biological functions of phosphatidylinositol transfer proteins. *Biochem. Cell Biol.* 82:254–262.

Schneggenburger, R., and E. Neher. 2005. Presynaptic calcium and control of vesicle fusion. *Curr. Opin. Neurobiol.* 15:266–274.

Selyanko, A.A., J.K. Hadley, I.C. Wood, F.C. Abogadie, T.J. Jentsch, and D.A. Brown. 2000. Inhibition of KCNQ1-4 potassium channels expressed in mammalian cells via M1 muscarinic acetylcholine receptors. *J. Physiol.* 522(Pt 3):349–355.

Seno, K., T. Okuno, K. Nishi, Y. Murakami, F. Watanabe, T. Matsuura, M. Wada, Y. Fujii, M. Yamada, T. Ogawa, et al. 2000. Pyrrolidine inhibitors of human cytosolic phospholipase A(2). *J. Med. Chem.* 43:1041–1044.

Shi, J., C.W. Heegaard, J.T. Rasmussen, and G.E. Gilbert. 2004. Lactadherin binds selectively to membranes containing phosphatidyl-L-serine and increased curvature. *Biochim. Biophys. Acta.* 1667:82–90.

Shi, X., P.G. Gillespie, and A.L. Nuttall. 2007. Apical phosphatidylserine externalization in auditory hair cells. *Mol. Membr. Biol.* 24:16–27.

Siegel, D.P. 1999. The modified stalk mechanism of lamellar/inverted phase transitions and its implications for membrane fusion. *Biophys. J.* 76:291–313.

Speight, P., and M. Silverman. 2005. Diacylglycerol-activated Hmunc13 serves as an effector of the GTPase Rab34. *Traffic.* 6:858–865.

Steinhardt, R.A. 2005. The mechanisms of cell membrane repair: a tutorial guide to key experiments. *Ann. N. Y. Acad. Sci.* 1066:152–165.

Steinhardt, R.A., G. Bi, and J.M. Alderton. 1994. Cell membrane resealing by a vesicular mechanism similar to neurotransmitter release. *Science.* 263:390–393.

Sugita, S., W. Han, S. Butz, X. Liu, R. Fernandez-Chacon, Y. Lao, and T.C. Sudhof. 2001. Synaptotagmin VII as a plasma membrane Ca^{2+} sensor in exocytosis. *Neuron.* 30:459–473.

Summers, S.A., B.A. Guebert, and M.F. Shanahan. 1996. Polyphosphoinositide inclusion in artificial lipid bilayer vesicles promotes divalent cation-dependent membrane fusion. *Biophys. J.* 71:3199–3206.

Sun, J., Z.P. Pang, D. Qin, A.T. Fahim, R. Adachi, and T.C. Sudhof. 2007. A dual-Ca^{2+}-sensor model for neurotransmitter release in a central synapse. *Nature.* 450:676–682.

Terasaki, M., K. Miyake, and P.L. McNeil. 1997. Large plasma membrane disruptions are rapidly resealed by Ca^{2+}-dependent vesicle-vesicle fusion events. *J. Cell Biol.* 139:63–74.

Togo, T., J.M. Alderton, and R.A. Steinhardt. 2000. The mechanism of cell membrane repair. *Zygote.* 8(Suppl 1):S31–S32.

Togo, T., J.M. Alderton, and R.A. Steinhardt. 2003. Long-term potentiation of exocytosis and cell membrane repair in fibroblasts. *Mol. Biol. Cell.* 14:93–106.

Toner, M., G. Vaio, A. McLaughlin, and S. McLaughlin. 1988. Adsorption of cations to phosphatidylinositol 4,5-bisphosphate. *Biochemistry.* 27:7435–7443.

Topham, M.K. 2006. Signaling roles of diacylglycerol kinases. *J. Cell. Biochem.* 97:474–484.

Tucker, W.C., J.M. Edwardson, J. Bai, H.J. Kim, T.F. Martin, and E.R. Chapman. 2003. Identification of synaptotagmin effectors via acute inhibition of secretion from cracked PC12 cells. *J. Cell Biol.* 162:199–209.

Wang, T.-M., and D.W. Hilgemann. 2008. Ca-dependent non-secretory vesicle fusion in a secretory cell. *J. Gen. Physiol.* 132:51–65.

Washington, N.L., and S. Ward. 2006. FER-1 regulates Ca^{2+}-mediated membrane fusion during *C. elegans* spermatogenesis. *J. Cell Sci.* 119:2552–2562.

Wei, S.K., J.F. Quigley, S.U. Hanlon, B. O'Rourke, and M.C. Haigney. 2002. Cytosolic free magnesium modulates Na/Ca exchange currents in pig myocytes. *Cardiovasc. Res.* 53:334–340.

Wienisch, M., and J. Klingauf. 2006. Vesicular proteins exocytosed and subsequently retrieved by compensatory endocytosis are nonidentical. *Nat. Neurosci.* 9:1019–1027.

Willig, K.I., S.O. Rizzoli, V. Westphal, R. Jahn, and S.W. Hell. 2006. STED microscopy reveals that synaptotagmin remains clustered after synaptic vesicle exocytosis. *Nature.* 440:935–939.

Wilschut, J., N. Duzgunes, and D. Papahadjopoulos. 1981. Calcium/magnesium specificity in membrane fusion: kinetics of aggregation and fusion of phosphatidylserine vesicles and the role of bilayer curvature. *Biochemistry.* 20:3126–3133.

Yaradanakul, A., S. Feng, C. Shen, V. Lariccia, M.J. Lin, J. Yang, T.M. Kang, P. Dong, H.L. Yin, J.P. Albanesi, and D.W. Hilgemann. 2007. Dual control of cardiac Na/Ca exchange by PIP2: electrophysiological analysis of direct and indirect mechanisms. *J. Physiol.* 582:991–1010.

Zeng, W.Z., X.J. Li, D.W. Hilgemann, and C.L. Huang. 2003. Protein kinase C inhibits ROMK1 channel activity via a phosphatidylinositol 4,5-bisphosphate-dependent mechanism. *J. Biol. Chem.* 278:16852–16856.

Zeniou-Meyer, M., N. Zabari, U. Ashery, S. Chasserot-Golaz, A.M. Haeberle, V. Demais, Y. Bailly, I. Gottfried, H. Nakanishi, A.M. Neiman, et al. 2007. Phospholipase D1 production of phosphatidic acid at the plasma membrane promotes exocytosis of large dense-core granules at a late stage. *J. Biol. Chem.* 282:21746–21757.